



Durham E-Theses

Experimental Analysis on Effectiveness of Confocal Algorithm for Radar Based Breast Cancer Detection

ABDUL-SATTAR, ZUBAIDA

How to cite:

ABDUL-SATTAR, ZUBAIDA (2012) *Experimental Analysis on Effectiveness of Confocal Algorithm for Radar Based Breast Cancer Detection*, Durham theses, Durham University. Available at Durham E-Theses Online: <http://etheses.dur.ac.uk/3531/>

Use policy

The full-text may be used and/or reproduced, and given to third parties in any format or medium, without prior permission or charge, for personal research or study, educational, or not-for-profit purposes provided that:

- a full bibliographic reference is made to the original source
- a [link](#) is made to the metadata record in Durham E-Theses
- the full-text is not changed in any way

The full-text must not be sold in any format or medium without the formal permission of the copyright holders.

Please consult the [full Durham E-Theses policy](#) for further details.



Durham
University

**Experimental Analysis on Effectiveness of Confocal Algorithm for
Radar Based Breast Cancer Detection**

By: Zubaida Abdul Sattar

Date: 6th February 2012

MSc by Research

University of Durham 2010/2011
School of Engineering, University of Durham,
Durham, United Kingdom.

TABLE OF CONTENTS

ABSTRACT	VI
ACKNOWLEDGEMENTS.....	VII
DECLARATION.....	VIII
1 INTRODUCTION.....	1
1.1 BACKGROUND.....	1
1.2 MOTIVATION.....	3
1.3 DISSERTATION OUTLINE	4
2 LITERATURE REVIEW.....	5
2.1 MORPHOLOGY OF BREAST	5
2.2 WHAT IS BREAST CANCER?	6
2.3 SYMPTOMS AND FACTORS LEADING TO RISK OF BREAST CANCER.....	7
2.3.1 BREAST TISSUE ELECTRICAL PROPERTIES.....	9
2.4 CURRENTLY USED SCREENING METHODS.....	10
2.4.1 X-RAY MAMMOGRAPHY.....	10
2.4.2 ULTRASOUND IMAGING.....	12
2.4.3 MAGNETIC RESONANCE IMAGING	13
2.5 COMPARISON BETWEEN SCREENING TECHNIQUES.....	14
2.5.1 COMPARISON OF X-RAY WITH ULTRASOUND & MRI TECHNIQUES.....	15
2.5.2 ULTRASOUND COMPARISON OVER X-RAY MAMMOGRAPHY	15
2.5.3 MRI COMPARISON OVER X-RAY MAMMOGRAPHY & ULTRASOUND.....	16
3 OVERVIEW OF MICROWAVE IMAGING.....	17
3.1 TYPES OF MICROWAVE IMAGING.....	17
3.1.1 PASSIVE MICROWAVE IMAGING	17
3.1.2 HYBRID MICROWAVE IMAGING.....	18
3.1.3 ACTIVE MICROWAVE IMAGING.....	19
3.2 MICROWAVE TOMOGRAPHY	20

3.3 UWB RADAR BASED MICROWAVE IMAGING	21
3.3.1 MIST SYSTEM	22
3.3.2 TSAR SYSTEM.....	23
3.3.3 CONFOCAL MICROWAVE IMAGING ALGORITHM.....	24
3.4 ASSESMENT OF MICROWAVE IMAGING TECHNIQUES & METHODOLOGY.....	26
4 EXPERIMENTAL SETUP FOR UWB PULSE RADAR	30
4.1 OVERVIEW.....	30
4.1.1 EXPLANATION OF EXPERIMENTAL SETUP	31
4.2 IMPLEMENTATION OF CONFOCAL ALGORITHM	35
4.2.1 PROCESS FLOW DIAGRAM OF ALGORITHM.....	35
4.2.2 EXPLANATION OF PROCESS FLOW	36
i TRANSFORMATION	37
ii CALIBRATION	38
iii CLUTTER REMOVAL.....	39
iv SYNTHETIC FOCUSING	40
v IMAGE	42
5 DISCUSSIONS & EXPERIMENTAL RESULTS.....	44
5.1 EXPERIMENTAL MEASUREMENTS	44
5.2 CONFOCAL ALGORITHM	46
5.3 ANALYSIS ON THE RESULTS	51
6 CONCLUSION & FUTURE IMPROVEMENTS	55
6.1 CONCLUSION.....	55
6.2 FUTURE IMPROVEMENTS	57
7 REFERENCES.....	58
APPENDICES.....	- 1 -
APPENDIX A: EXPERIMENTAL SETUP COMPONENT PICTURES	- 1 -
APPENDIX B: MATLAB CODE	- 3 -
APPENDIX C: PRESENTED PAPER & CERTIFICATE IN URSI FESTIVAL 2011.....	- 6 -

LIST OF FIGURES

Figure 1-1 Principle of tumour detection in breast.....	3
Figure 2-1 Anatomy of breast (a) Front view (b) Side View.....	5
Figure 2-2 Most Commonly Diagnosed Cancers in Females, UK 2008.....	7
Figure 2-3 Death rate due to breast cancer amongst males and females with different age groups UK 2008	8
Figure 2-4 X-Ray mammography imaging unit.....	11
Figure 2-5 Ultrasound imaging system	12
Figure 2-6 Magnetic resonance imaging machine	14
Figure 3-1 Passive microwave imaging	18
Figure 3-2 Hybrid microwave imaging	18
Figure 3-3 Methods of breast imaging at microwave frequencies (a) Passive approach involving the detection of area of increased temperature which corresponds to tumor (b) Hybrid methods heat with microwaves (c) Active approaches with illumination of breast with microwaves (d) Patient orientation planar (e) cylindrical system	19
Figure 3-4 The imaging system of Dartmouth college with 16 antenna array position in a circular setup	20
Figure 3-5 (a) Prone and (b) Supine Position for MIST System at the University of Wisconsin.....	22
Figure 3-6 Patient to be imaged lies on her stomach with the breast extending through a hole in the examination table.....	23
Figure 3-7 Planar configuration	25
Figure 3-8 Cylindrical configuration	25
Figure 3-9 A representation of mono-static confocal imaging algorithm...	28
Figure 4-1 Modified experimental setup.....	32

Figure 4-2 Process flow diagram of algorithm35

Figure 4-3 Antenna positions covered in an area of 100mm by 100mm...37

Figure 4-4 Pixel point locations for Synthetic focusing to find time values
.....40

Figure 4-5 Representation of finding the round trip distance of each
Antenna position to the pixel points.....41

Figure 4-6 (a) Image using 2nd Power.....43

Figure 4-6 (b) Image using 4th Power43

Figure 5-1 Scattering parameters measured in Environment45

Figure 5-2 Scattering parameters measured in Environment in the
presence of Breast Phantom45

Figure 5-3 (a) Illustration of Environment Signal with hamming window
.....45

Figure 5-3 (b) Response of Environment Signal after applying
hamming window.....45

Figure 5-4 Response of Environment Signal after applying IFFT46

Figure 5-5 Response of Tumour Signal after removing the
Antenna Backscatter47

Figure 5-6 (a) Image of intensities for wood as tumour at 1cm distance....47

Figure 5-6 (b) Image of intensities for wood as tumour at 3cm distance ...47

Figure 5-7 (a) Image of intensities for water as tumour at 1cm distance....48

Figure 5-7 (b) Image of intensities for water as tumour at 3cm distance ...48

Figure 5-8 (a) Image of intensities for copper as tumour at 1cm distance .48

Figure 5-8 (b) Image of intensities for copper as tumour at 3cm distance .48

Figure 5-9 (a) Image of intensities for PVC as tumour at 1cm distance.....49

Figure 5-9 (b) Image of intensities for PVC as tumour at 3cm distance.....49

Figure 5-10 (a) Image of intensities for glass as tumour at 1cm distance ..49

Figure 5-10 (b) Image of intensities for glass as tumour at 3cm distance49

Figure 5-11 (a) Image of intensities for plastic as tumour at 1cm distance50

Figure 5-11 (b) Image of intensities for plastic as tumour at 3cm distance50

Figure 5-12 (a) Image of intensities for rubber as tumour at 1cm distance50

Figure 5-12 (b) Image of intensities for rubber as tumour at 3cm distance50

Figure 5-13 Intensity of different Materials for antenna at a distance of 1cm 51

Figure 5-14 Comparison of Intensities of materials at 1cm & 3cm depth of tumour 52

Figure 5-15 Signal strength received at the antenna for water as tumour at 1cm and 3cm depth..... 53

Figure 5-16 Effect of permittivity of medium in detecting tumour using Confocal Algorithm..... 54

Abstract

Breast cancer is one of the most commonly diagnosed cancers in females in UK [1]. Early breast cancer detection which has recently been gaining a lot of consideration within the research community and the most important for a quick and effective treatment of the cancer is early detection. UWB radar based microwave imaging for early breast cancer detection is one of the most promising and attractive screening techniques currently under research. This technique offers several advantages such as low cost, better patient comfort, non-ionising and non-invasive radiation compared to X-Ray mammography. In this technique the breast is illuminated from various points with short UWB microwave pulse(s) and the collected backscattered energy is then processed to identify the presence and location of the tumour.

In this thesis experimental measurement of the reflection coefficient in complex frequency domain is obtained from Vector Network Analyzer (VNA E5071) when the antenna is exposed to the environment and when the antenna is exposed to breast phantom. The tumor is simulated with different materials to investigate the effectiveness of the Confocal Microwave Imaging Algorithm for breast cancer detection. In addition, we used the materials at different depths to determine the effect of antenna distance to that of the tumor response.

The Confocal Microwave Imaging (CMI) Algorithm for breast cancer detection is an easy and robust technique for tumor detection, which is used to approximate the precise location of the tumor. CMI is based on illuminating the breast with the UWB pulse from different antenna locations. The relative arrival times & amplitudes of the backscatter signals is used to estimate the location of the tumor. We applied the Confocal Algorithm in this study to the numerical data generated with the VNA and analyzed the results with different material(s) as tumor at different depth to verify its ability to estimate a tumor response.

Acknowledgements

First and foremost I would like to thank Allah (God) for all what I am and all what I have. I would like to thank my supervisor Prof. Sana Salous for the valuable guidance and advice. She has inspired me greatly to work in this project and has helped me with new techniques to make this project successful. Then I would like to offer my kind regards to those who supported me during this research endeavor. Besides, I would like to thank the authority of Durham University for providing a good environment and facilities. This project provided the knowledge of different facts and figures for a Breast cancer patient, and its research has provided with its awareness and the knowledge on how to reduce the adverse effects.

I would like to pay my gratitude to my “Memon Communities” (**Euro Charity Trust; World Memon Organization; The Jetpur Memon Higher Educational Welfare Trust; Aziz Tabba Foundation and Adamjee Foundation**) which has provided me with the funding to study in such a prestigious University worldwide. Lastly I would thank my Family specially my parents, for supporting me with my career move.

Declaration

No portion of the work referred to in this report has been submitted in support of an application for another degree or qualification at this or any other university, or institution of learning.

1 INTRODUCTION

1.1 Background

Breast cancer has become one of the most widespread diseases worldwide making it a threat to the women of our society [2-9]. The technological boom in every aspect has made researchers to ponder over a screening tool that can be used to detect tumor in its developing stage, which can be used by the surgeons for further diagnosis [10].

Researchers have been trying to develop a way to utilize non-ionizing electromagnetic waves to image the human body in order to detect cancer. Recently, significant progress has been made towards breast cancer detection [3]. In the advent of ten years it is likely that microwave systems will become a possible solution. Breast tumors have electrical properties at microwave frequencies, which are different in contrast to healthy or normal breast tissue [11]. X-Ray being a known technology to detect breast cancer has reportedly caused side-effects to the breast tissues of the patient under examination. Researchers have implemented ultra wide band radar based microwave imaging techniques, and have found it to be a potential modality for early detection of breast tumor in the recent years to come and the advantages can be noted as follows [3]:

- Low cost implementation;
- Exposure to non-harmful radiation;
- High accuracy;
- Better patient comfort compared to the currently used X-Ray mammography.

In spite of the benefits of using Ultra Wideband pulses, it presents many challenges. Particularly in,

- Hardware & antenna design;
- Imaging algorithm.

According to the IOM (U.S. Institute of Medicine) report, an ideal breast screening tool [12]

- Has minimal health risk;
- Sensitive to tumors;
- Early cancer detection capability
- Non-invasive and easy to perform
- Cost effective, easy to understand & consistent
- Provides minimum discomfort to patients

For detection of small tumor(s), a consistent contrast between tumor and normal breast tissues is required. Medical imaging methods have been applied to breast cancer detection with various degrees of success [12]. Ultrasound is used to determine whether the detected lesion is a liquid cyst or a solid tumor. Magnetic resonance imaging, is useful to examine embedded tumors, but expensive as a screening tool [12]. Methods to detect cancerous tissues are based on different physical properties being, tissue elasticity, temperature, and optical or electrical characteristics. We are particularly interested in techniques that employ electrical property contrasts. Active approaches for breast tumor detection are currently being researched in the microwave frequency range.

Ultra-wideband (UWB) Radar imaging of the breast uses the difference in dielectric strengths of normal and cancerous tissue, in microwave frequency ranges [7]. In general UWB imaging algorithms use an UWB pulse which illuminates the breast and then the backscattered signals are measured. Imaging techniques are then applied on the backscattered signal to construct an estimated image of the examined breast tissue [13].

Figure 1-1 shows the basic principle of tumor detection in a breast where a signal is transmitted through an antenna and the received signal is then processed to determine the location and size of tumour.

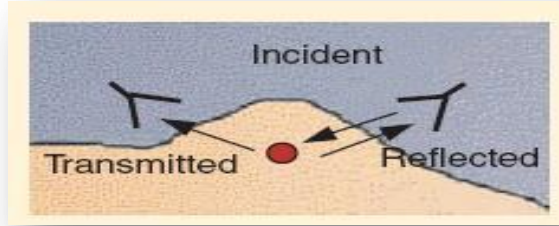


Figure 1-1: Principle of tumour detection in Breast [3].

A number of imaging algorithms have been presented by many researchers. In this report experimental results of UWB microwave imaging system for radar-based breast cancer detection were obtained to evaluate the effectiveness of Confocal Microwave Imaging Algorithm with different materials as tumor.

1.2 Motivation

The dissemination of breast cancer disease is reported to increase rapidly due to the shortcomings in the currently used screening methods, where X-ray mammography is the widely used screening technique amongst MRI and Ultrasound to detect breast tumors however it has been reported to have estimated false results for around 30% of women who have had a screening [7-8]. The considerable amount of false results obtained is noticeably the limitation of the present screening methods in analyzing dense breast tissue and the area where the tumor might be located close to the chest or under the arm and mainly the estimation of early stage tumors [14]. Nowadays, researchers are employing microwave imaging techniques for non-invasive testing of breast cancer. The presence of tumor is being detected by comparing the dielectric properties of cancerous and normal breast tissues for detecting breast cancer.

The motivation of using the microwave techniques to diagnose a patient with breast cancer at the early stage is beneficial. In this thesis we demonstrate the experimental setup to review the confocal imaging algorithm which is used in radar based breast cancer detection with high concern in reducing the amount of clutter in the backscatter signal(s) to investigate its effectiveness for different materials as tumor. In addition, we use the materials at different depths to identify the effect of antenna distance to that of the tumor response.

1.3 Dissertation Outline

The remainder of this dissertation is composed of 6 chapters. Each chapter is a self-contained report on an aspect of breast cancer detection. In this section we provide a brief overview of the chapters.

Chapter 2 discusses the review of the imaging techniques currently being used and their advantages and disadvantages and discusses why microwave imaging is being considered in recent years and the comparison between the screening techniques with their limitations.

Chapter 3 overviews the microwave imaging methods and discusses the current imaging techniques being employed as research in different parts of the world with insight knowledge of the imaging algorithms being used. Assessment of microwave imaging techniques and methodology is discussed in the end.

Chapter 4 discusses the experimental setup of the current research held at Durham University, and explains the critical parameters involved in confocal microwave imaging algorithm used in detecting different materials as tumor.

Chapter 5 provides the discussion on the experimental results obtained.

Chapter 6 gives the conclusion and future improvements in target to achieve a standalone non-invasive screening method for breast tumor detection.

2 STUDY ON BREAST CANCER & SCREENING METHODS

2.1 Morphology of Breast

Screening tools require a study and understanding of the internal structure of breast to develop an efficient tool. Figure 2-1 defines morphological structure of the female breast [15].

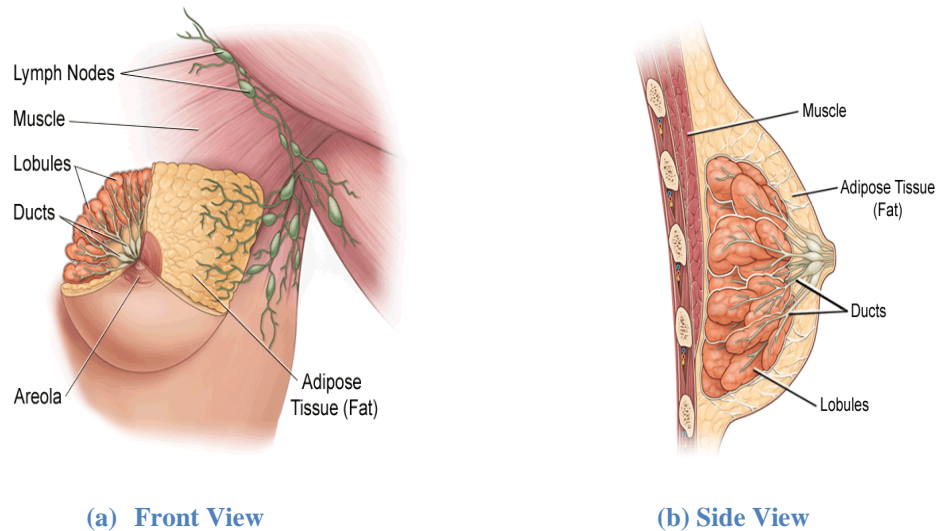


Figure 2-1 Anatomy of Breast [15]

The breast is divided into the following main sections [16].

➤ Breast Gland

- Each breast has 15 to 20 sections (lobes) arranged like the petals of daisy;
- Inside each lobe are many smaller structures called lobules ;
- At the end of each lobule are tiny sacs (bulbs) that can produce milk;

➤ Ducts

- Lobes, Lobules and bulbs, are linked by a network of thin tubes (ducts);
- Ducts carry milk from bulbs towards the dark area of skin in the center of the breast (areola);
- Ducts join together into larger ducts ending at the nipple, where milk is delivered;

➤ Lymph nodes: Filter harmful bacteria and play a key role in fighting off infection.

There are no muscles in the breast, but muscles lie under each breast and cover the ribs. Each breast also contains blood vessels and vessels that carry lymph. The lymph vessels lead to small bean-shaped organs called lymph nodes, clusters of which are found under the arm, above the collarbone, and in the chest, as well as in many other parts of the body [17].

2.2 What is Breast Cancer?

Breast cancer is a malignant tumor that has developed from cells of the breast. A malignant tumor is a group of cancer cells that may invade surrounding tissues or spread to distant areas of the body [1].

The incidence of breast cancer in women is very low in the twenties and gradually increases and plateaus at the age of forty-five and increases dramatically after fifty, where fifty percent of breast cancer is diagnosed in women over sixty-five indicating the ongoing necessity of yearly screening throughout a woman's life [1]. The disease occurs almost entirely in women, but men can get it, too.

For every 100 women with breast cancer, 1 male will develop the disease. The information on this page refers only to Breast Cancer in women. Figure 2-2 shows the percentage of diseases recorded

by the cancer research UK signifying that at least 31% women diagnosed with cancer have breast cancer.

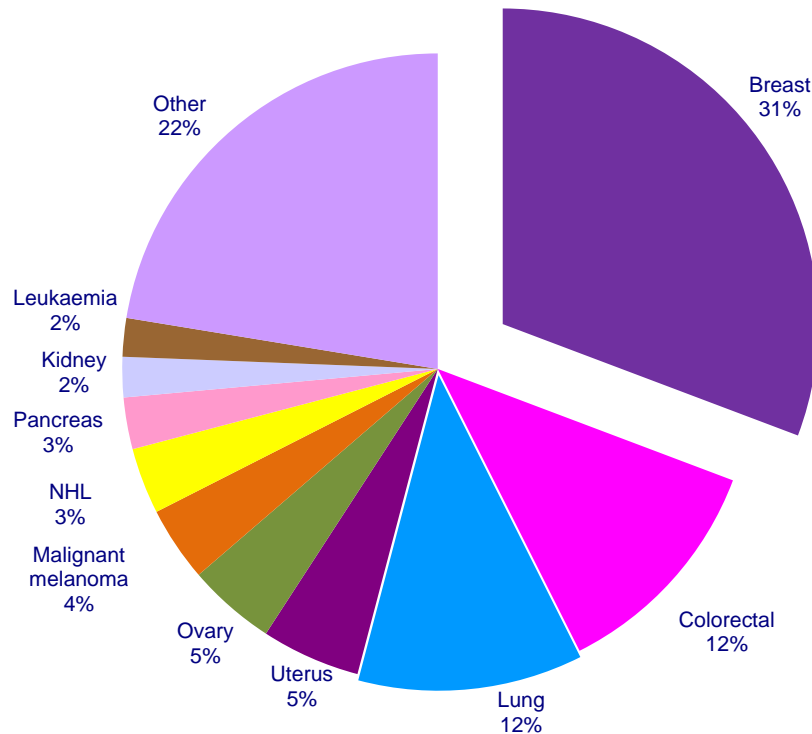


Figure 2-2 Most Commonly Diagnosed Cancers in Females, UK 2008 [1]

2.3 Symptoms and factors leading to Risk of Breast Cancer

Breast cancer is considerably the most commonly diagnosed cancer in females with an age-standardized (a technique used to better allow populations to be compared when the age profiles of the populations are quite different) rate of 124 per 100,000 females, accounting for almost 1/3 of all women cases in UK. According to the statistics of 2009 breast cancer claimed around 12000 lives every year in the UK, and it is the second most common cause of death from cancer in women after lung cancer [1].

A patient bearing breast cancer, the surrounding cells are affected and in a span of time it can damage the breast tissues of the human body. Major signs include the indication of red marks

around the breast, discharge of blood from the nipples, nipple turning inward, and pain in the breast [1].

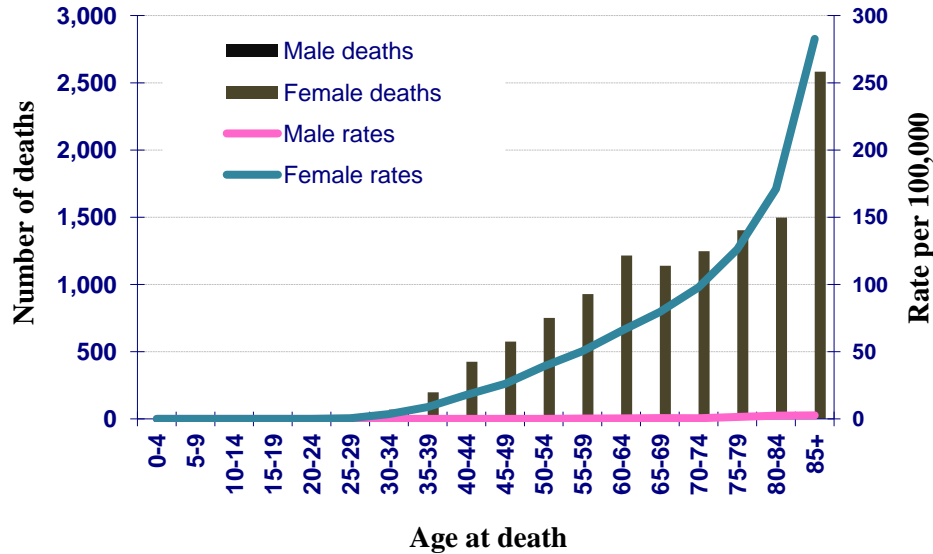


Figure 2-3 Death Rates due to Breast Cancer amongst males & females with Different age group, UK 2008 [1]

Figure 2-3 show the rate of increase in death related to breast cancer in males and females. The major risk, besides the symptoms mentioned is the spreading of cancer in the surrounding cells (the lymph nodes) even before any sign of cancer is evident. There are several risk factors that cause breast cancer. The following are the known risk factors and causes of breast cancer [1]:

- ***Inheritance***

Breast cancer is more risky for women whose close relatives has or had a breast cancer.

- ***Abortion***

Doctor(s) investigation leads to the conclusion that women who have had an abortion at a young age have a high risk for breast cancer.

- ***Growth***

The chance of getting breast cancer goes up as a woman gets older. It has been surveyed that the women at the age of 50 to 64 are diagnosed with breast cancer.

- **Weight**

Overweight or obesity of women has a huge risk of developing breast cancer.

2.3.1 Breast Tissue Electrical Properties

Microwave interaction with the human body tissues cause the electromagnetic wave's amplitude to change as it propagates through it, or disperses from the body tissues. Research into the electrical properties of human body tissues at microwave frequency range (300MHz – 300GHz) dates back more than 50 years ago [18-19]. Body tissues electrical properties are represented in terms of relative permittivity (ϵ_r) and conductivity (σ). In all these studies tissues permeability (μ) is often ignored and assumed to be that of free space, possibly due to the fact that human body tissues are considered to be nonmagnetic material.

Studies revealed that tissues permittivity are highly dependent on the water content; low water content tissues (such as fat) have lower permittivity than high water content tissues like: muscle, skin, heart, and cancer tissues [11,18-19]. While permittivity gives us the indication of the tissues ability to store microwave energy, conductivity on the other hand is related to the loss (dissipation) or attenuation (absorption) the signal suffers as it propagates through the tissue. High conductivity tissue causes higher loss or attenuation to the microwave signal. Therefore, as the microwave signal travels through different tissues on the breast it suffers both attenuation (amplitude loss) and reflection as it encounters discontinuity.

Understanding the electrical properties and heterogeneities of the female breast are important as it aids in the creation of more realistic either numerical or physical breast phantoms that can be used to access the efficacy of any microwave imaging technique for diagnoses and detection of cancer. Measurements on the tissue electrical properties depend on a number of factors such as: tissue density, temperature, water content, location on breast, etc.

2.4 Currently Used Screening Methods

Research and surveys for breast cancer detection have been studied and conducted by most of the researchers worldwide, and different procedures and detection tools have been utilized by them. Breast cancer can be diagnosed by one of the following techniques.

- X-ray Mammography
- Ultra-Sound
- MRI

The X-ray (Screening) Mammography is conducted on women with no symptoms of breast cancer, and if a women is diagnosed with a cancerous tissue or an abnormality is found, an ultrasound screening is carried out. If both of the screening methods fail to produce any significance for the formation of the signs of breast cancer, medical biopsy is carried out where by a sample of breast tissue is removed by a surgeon and tests are carried out in order to determine whether the tissue is cancerous or healthy. The aforementioned existing screening tools with their advantages and disadvantages are as follows [20-26].

2.4.1 X-Ray Mammography

X-ray mammography is currently the most recommended method utilized by doctors for breast cancer examination. This technique involves compressing the breast between two plates. X-rays emission, are then passed through the breast and recorded onto film. Figure 2-4 shows an X-ray system [27]. X-ray mammography uses ionizing radiation which is harmful. The breast is compressed onto plastic plates which is reportedly painful to the patient.



Figure 2-4: X-Ray Mammography Imaging Unit [27]

a. Advantages

- i. Good sensitivity.
- ii. High-quality resolution.
- iii. Time to form an image is short.

b. Disadvantages

- i. Not enough sensitivity for patients having dense (thick) breast tissues.
- ii. It is hard to analyze the contrasts of mammogram because the physical appearance of breast for each patient is not the same.
- iii. The breast is compressed between the plates which is painful for the patient.
- iv. Unsafe and harmful because of the ionizing radiations used in the process.

2.4.2 Ultrasound Imaging

Ultrasonic waves for diagnosing an internal body structure, comprises of non-harmful radiation with a frequency range of 1MHz to 15MHz. It determines whether the area under consideration consists of a cancerous tissue or not. For a solid tissue found in the testing, it will require a biopsy to be conducted to verify if it is cancerous in nature. In addition, Ultrasound imaging can be made from any angle or orientation. Figure 2-5 shows an Ultrasound Imaging System [27].



Figure 2-5: Ultrasound Imaging System [27]

a. Advantages

- i. Safe screening tool because there is no harmful radiation.
- ii. Detection and examination for young women with dense breasts and women with breast implants are applicable.
- iii. Image contrast and resolution is high which yields a high distinction between normal tissue and suspicious areas.

b. Disadvantages

- i. System performance is dependent on the technician's skills and the operator expertise.
- ii. Some solid masses cannot be distinguished.
- iii. Deep lying lesions can barely be detected.

2.4.3 Magnetic Resonance Imaging

Magnetic Resonance Imaging (MRI) is a non-invasive technique which uses strong and powerful magnets and radio waves to form images. It is able to distinguish a soft tissue to a brittle one. MRI operates at high frequencies, and to avoid any interference of the environmental clutter, the system is placed in a protected and shielded room.

The patient under examination has to lie down on a table as shown in Figure 2-6 [27]. In addition small scanners or devices are placed around the breast to examine and to enhance the quality of the image yet to be formed. For a single test, several images are usually required in order to complete a test, which takes hours and is time consuming. The machine produces loud pounding and buzzing noises during the operation. To help reduce the noise, patients are provided with ear caps.



Figure 2-6: Magnetic Resonance Imaging Machine [27]

a. Advantages

- i. Patients with dense breasts can be examined effectively using MRI.
- ii. Non-ionizing imaging technique.
- iii. Images can be captured from different orientations.
- iv. Capability of detecting small tumors.
- iv. Multi-focal cancers can be detected.

- v. Helpful in determining if the cancer reaches the chest wall.
- vi. Breast implants and ruptures can be detected.

b. Disadvantages

- i. Extremely expensive.
- ii. Immobile and fixed.
- iii. Injection of a contrast agent for operative testing is needed.
- iv. Calcifications cannot be detected.
- v. Patient feels a fear of being in a narrow space (claustrophobia).
- vi. Time consuming as compared to X-ray and ultrasound scanning technique.

2.5 Comparison between screening techniques

Early detection and diagnoses of breast cancer has proven to largely improve the chance of a quick and successful treatment as well as patient long term wellbeing. X-ray mammography, Ultrasound and MRI are the screening techniques which are used for breast cancer detection, the comparison between these techniques are as follows [20-26]:

At the moment, the most common technique used in breast cancer detection is X-ray mammography which is the primary method for early stage breast cancer screening. During the screening the breast is compressed firmly between two plastic plates and an X-ray image is formed. As compared to other techniques X-ray mammography offers several advantages such as High-quality resolution of image, detection sensitivity is high, and the time to the formation of an image is short as well. However this technique has several drawbacks over other screening technique(s) which is discussed in sections 2.5.1 to 2.5.3.

2.5.1 Comparison of X-ray with Ultrasound and MRI Techniques

X-ray Mammography has several drawbacks over Ultrasound and Magnetic Resonance Imaging (MRI) screening techniques, such as the extreme pain because X-ray mammography involves

compressing the breast between two plates and thus recording the image onto film which is painful to the patient and causes discomfort due to the breast compression and it is also not efficient for patients having dense (thick) breast tissues.

Moreover the screening technique is relatively expensive and causes potential damage to the breast since it is exposed to ionizing radiation which is harmful for breast tissues. Most important, it has difficulties in detecting early and small breast tumors and also in detecting tumors located near the chest wall or arm. In addition it is hard to analyze the contrasts of mammogram because the physical appearance of breast for each patient is not the same.

2.5.2 Ultrasound comparison over X-ray Mammography

Ultrasound testing uses Ultrasonic waves for diagnosing an internal body structure, with a frequency range of 1MHz to 15MHz. As compared to X-ray mammography, Ultrasound is a safe screening tool because it comprises of non-harmful radiation which does not cause discomforts to the patient and that the detection and examination for young women with dense breasts and women with breast implants are applicable using Ultrasound as a screening technique.

The image contrast and its resolution are high as in the case of X-ray mammography which yields a high distinction between normal tissue and suspicious areas although the tumor laying deep down the breast are hard to detect in Ultrasound. It is also hard to distinguish between a solid mass with that of a solid tissue, and therefore to discriminate them a biopsy is required to verify whether its nature is cancerous or healthy. The overall system performance of Ultrasound is dependent on the technician's skills and the operator expertise which is a drawback as compared to X-ray Mammography.

2.5.3 MRI comparison over X-ray Mammography and Ultrasound

Magnetic Resonance Imaging (MRI) is a non-invasive technique that uses strong and powerful magnets to produce radio waves in order to generate images as compared to X-ray mammography. Due to the powerful magnets the sensitivity of distinguishing soft tissues with brittle one(s) is high as compared to Ultrasound. Patients having dense breasts can be examined effectively using MRI

and the safe non-ionizing radiation helps in detecting tumor without causing any side effects as compared to X-ray mammography.

Images can be captured from different orientations to estimate the precise location of tumor and due to which it can also detect multi focal cancers. Due to its higher sensitivity it is also capable of detecting small tumors as compared to X-ray mammography and Ultrasound. MRI screening is helpful in determining if the cancer reaches the chest wall, and that breast implants and ruptures can also be detected. Apart from its sensitivity and capability of detection tumors it has certain shortcomings.

Since MRI screening requires a big area for the machine to be placed, which makes it fixed and it is hard to be replaced to another location, which makes it not suitable for large-scale screening programs. It requires contrasting agents which is used to improve the visibility of internal body structure in MRI screening (the most commonly used compounds for contrast enhancement are gadolinium-based) which is injected for operative testing. For an MRI screening, patients have to lie down inside a large cylindrical structure during the scanning process which may cause a claustrophobic effect on patients due to the fear of being in a narrow compartment.

These limitations have generated an immense interest in the development of a more effective and cheaper alternative tool for early detection and diagnoses of breast cancer. Over decades a number of research groups have been proposing microwave imaging as the imaging method for early breast cancer detection and diagnoses. Microwave imaging offers the potential for low cost scanners, non-invasive, harmless and within non-ionizing frequency range which is discussed in chapter 3.

3 OVERVIEW OF MICROWAVE IMAGING TECHNIQUES

Microwave imaging has been of interest for many years for tumor detection. The advantage of microwave imaging includes wide range of frequencies, capability to focus the energy, ranges of simulation tools, less health risk and less expensive. Presently, microwave imaging for early tumor detection has successfully gained attention due to the current advancements in imaging algorithms. Microwave imaging is a non-ionizing technique which is without doubt inexpensive compared to MRI and X-ray, and therefore is considered as an alternative imaging technique for breast cancer detection in the future [5].

3.1 Types of microwave imaging

Three types of microwave imaging techniques, namely passive, hybrid, and active approaches, for breast cancer detection are discussed [3, 7 - 9, 13 - 14, 28 – 31, 46].

3.1.1 Passive microwave imaging

Passive microwave imaging involves measuring the contrast between the temperatures of the cancerous tissue to that of the normal one. Evidence of the difference in temperature in the presence of cancer tissues has been reported by several investigators examining patients with breast cancer, where it is concluded that the cancerous tissues are more active and produce more heat [3, 46]. It is further established that tumors may not have the thermoregulatory capacity (ability of tissues to keep its temperature within certain boundaries) that of normal tissues [3].

In Passive Microwave Imaging technique radiometers are used to measure the temperature differences in the breast to detect the presence of cancerous tissue in breast. Under the illumination of the microwave radiation the tumor shows a greater increase in temperature compared with normal breast tissue. This technique basically measures and maps the change in temperature observed at the surface of the breast to the physical change in temperature at the considered location in the tissue. Figure 3-1 shows this kind of imaging system.

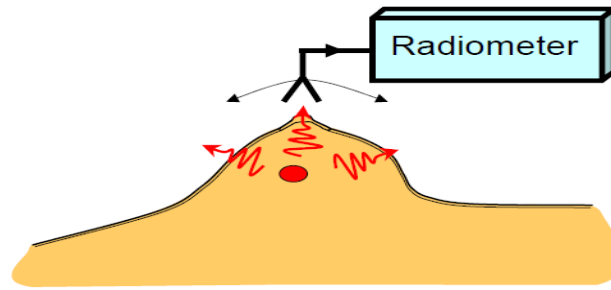


Figure 3-1: Passive Microwave Imaging [46]

3.1.2 Hybrid microwave imaging

For the hybrid technique, microwave energy is illuminated on the breast and then pressure waves due to the expansion of heated tumors are detected. This approach provides sensitivity to tumors and high resolution images. Tumor having higher conductivity absorbs more microwave energy as compared to the normal tissue thus producing stronger pressure waves. Hybrid (acoustic) microwave imaging systems use microwaves to rapidly heat selected areas in the breast, and to detect the pressure waves generated by the expansion of the heated tissues ultrasound transducers are used. Under the illumination of the microwaves, more energy is deposited in tumors in comparison to normal breast tissue. Further details of this technique can be found in [3]. Figure 3-2 shows an illustration of the principal of hybrid system.

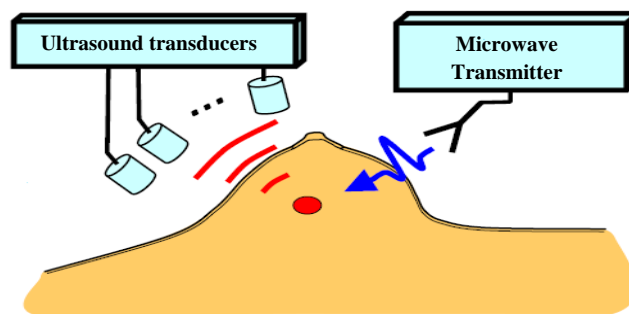


Figure 3-2: Hybrid Microwave Imaging [46]

Apart from the passive and hybrid imaging techniques, active microwave imaging technique have proved to achieve promising results in early breast cancer detection which is discussed in section 3.1.3 of the report.

3.1.3 Active microwave imaging

Active techniques of microwave imaging have been of interest for many years. As discussed above, these methods rely also on the significant electrical properties and contrast between malignant and normal breast tissues at microwave frequencies. The three different approaches for microwave breast imaging are illustrated in Figure 3-3.

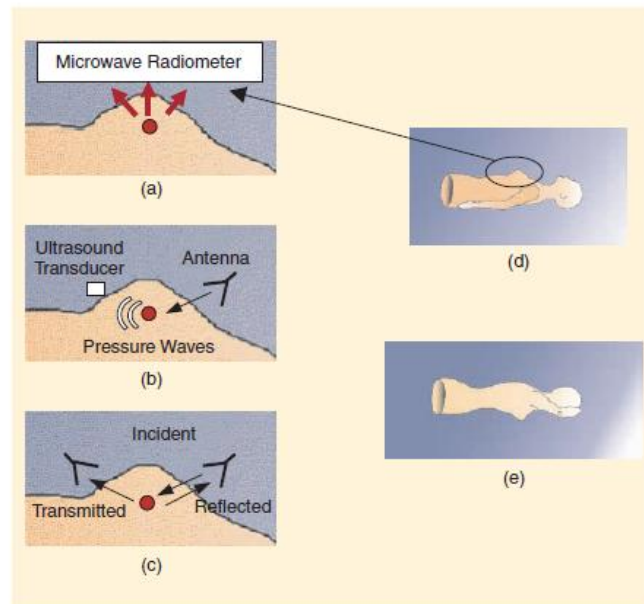


Figure 3-3: Methods of breast imaging at microwave frequencies. (a) Passive approaches involve detecting areas of increased temperature, which correspond to tumours. (b) Hybrid methods heat with microwaves. Ultrasound transducers detect the pressure waves generated by tissue expansion. (c) Active approaches involve illuminating the breast with microwaves and then forming images with energy transmitted through or reflected from the breast. The figures on the right show patient orientations for (d) planar and (e) cylindrical systems. [3]

For breast imaging, active microwave techniques are classified as **microwave tomography** and **radar-based microwave imaging**. The mentioned approaches use, low-power microwave signals which are transmitted into the breast using a set of antennas, which in turn, uses the backscatter signals to form the image. These techniques have achieved promising results.

3.2 Microwave Tomography

Microwave Tomography imaging technique, uses multiple signals collected from sensors (antennas) at different positions (locations) received from the surface of the breast. These collected signals (measured data) are then used to determine the level of permittivity inside the breast in order to create a dielectric trace, consisting of the physical and electrical properties of the breast. The dielectric profile is established by a number of inverse scattering problems [9].

Microwave tomography approach was introduced at the Dartmouth College. It uses narrowband signals and the scattered signals received by antennas to create a trace of electrical properties of the breast using algorithms that basically match measurements of the microwave signal scattered by the breast to results computed with a model. The existence of tumors reduces the strength of the scattered signal, which results in areas of increased permittivity and conductivity on images.

The system employed at the Dartmouth College shown in Figure 3-4 consists of a 16 multi-static antenna array for measurements and an inverse scattering algorithm with an operating range of 0.5 to 2.3 GHz [32].

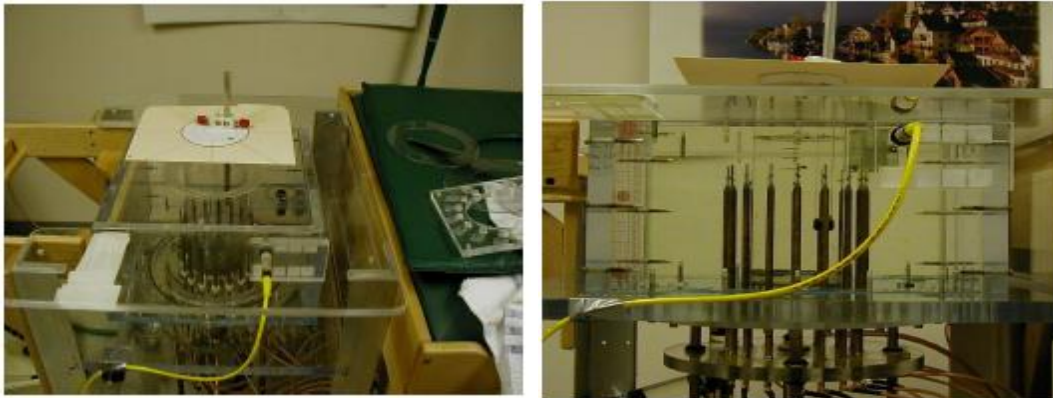


Figure 3-4: The Dartmouth College microwave imaging system. [32].

The clinical system shown in Figure 3-2 examines the patient lying with the breast pendant through a hole in the examination table and immersed in a tank. This tank is filled with glycerin water as a coupling liquid to reduce the environment clutter that affects the measurements as the antenna is placed at a distance from the breast. The ratio of the glycerin and water is varied in order to match the properties to that of the breast whether it is fatty or dense.

The antennas used were simple monopoles. The sensors are rotated vertically for seven times to record seven measurements at each position in order to cover the entire region of the breast. At each position an antenna act as a transmitter while the remaining act as receivers, thus generating a total of 240 measurements. The measurements are further used to generate the dielectric profile. A more detailed literature of the system can be found in [33-35].

3.3 UWB Radar Based Microwave Imaging

The existing screening modalities being used and their limitations lead to the interest in developing a consistent and cost effective solution for early detection of breast tumor. For the past 10 years, researchers have proposed novel and persistent imaging methods to be applied clinically to detect breast cancer. UWB Radar based Microwave Imaging technique is being used by most of the researchers to develop a potential screening modality which is not limited as the previously discussed methods mentioned in section 2.4.

The main feature of this technique is to signify the use of dielectric properties of a breast tissue to picture out the contrast between the cancerous and healthy tissue. As the electromagnetic signal is illuminated the signal is absorbed or back scattered. This scattering is used to form a map like image to distinguish the position of the strong reflections. Tumor detection using UWB Radar does not attempt to recreate the dielectric properties of the breast but concentrates on detecting and focusing the existence of a strong reflection.

Hence, the approach makes it computationally more efficient than microwave tomography, whereby the dielectric properties of the breast are recreated [34]. Dartmouth College has given an approach to this technique. The UWB radar uses a short pulse, to illuminate the breast to get the information in the reflected scatter. The received or the reflected signal also termed as backscatter in radar terminology is processed to generate a pictorial view showing the location and the position of the scatter.

3.3.1 MIST System

Microwave Imaging via Space Time (MIST) beam-forming system was introduced by **Hagness et al** in the University of Wisconsin [7]. In the system, the following arrangements are considered as shown in Figure 3-5.

- i. Breast screening of a woman lying in flattened position, where an antenna array is placed on the surface of the breast.
- ii. Breast screening of a woman in the pendant position, with the breast extending through an opening in a treatment table.

In this method, the breast is illuminated with the UWB pulse throughout the synthetic focus from point to point within the breast to create an image.

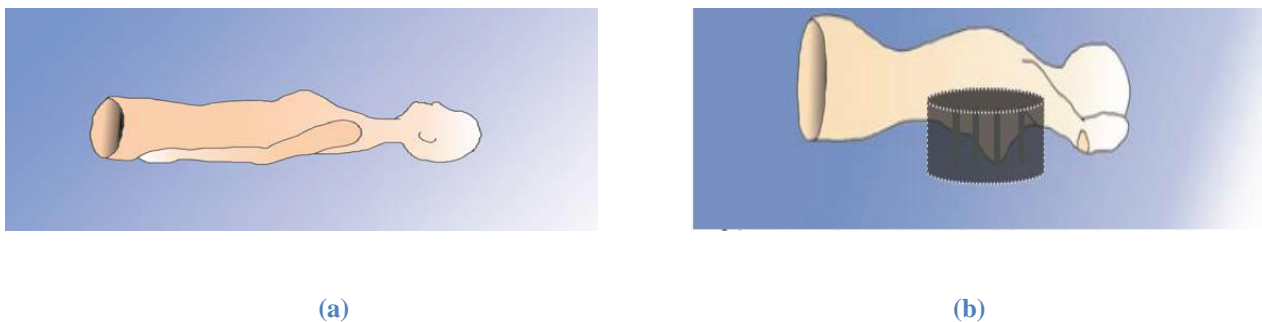


Figure 3-5 (a) Prone & (b) Supine Position for MIST System at the University of Wisconsin [7]

To create an image at a given position in the breast, the received signals need to be processed. Following the received signal the Confocal Microwave imaging algorithm is applied which is discussed later in chapter 4.

3.3.2 TSAR System

The Tissue Sensing Adaptive Radar (TSAR) system was developed at the **Universities of Calgary and Victoria** [9]. The approach is similar to that discussed in MIST where the breast is subjected into a hole in the examination table. In the system the breast extends into a tank containing a calibration liquid and an antenna. The purpose of using the calibration liquid is to suppress the electrical differences between the environment and the breast in order to reduce the amount of clutter for better results.

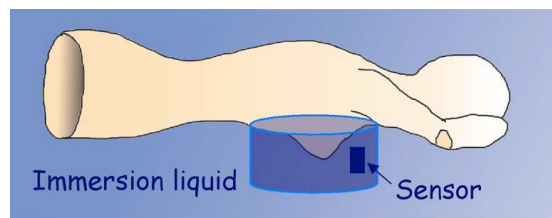


Figure 3-6: Patient to be imaged lies on her stomach with the breast extending through a hole in the examination table [9]

In TSAR a mono-static (single) antenna is used to perform the scan, where the antenna is rotated around the breast to create an antenna array as shown in Figure 3-6. The antenna is placed approximately 1 cm from the breast. Further clutter suppression is carried out using sophisticated computational algorithm to create an image. The main approach is that the breast is first located, and then the skin reflections are identified to approximate the skin response from the signal. Then this response is subtracted from the received signal and focusing is applied to create a map of the precise location of the tumor.

In order to improve the TSAR system, currently new and appropriate designs of sensors are being made with a high concern on the imaging algorithm to reduce computational time and the feasibility of creating a system to test on breast models.

3.3.3 Confocal Microwave Imaging Algorithm

Confocal or the Delay-and-Sum Imaging Algorithm is mostly applied as part of UWB systems in recent years [8,13 - 14, 28, 31]. The concept for utilizing CMI for breast cancer detection was first introduced by **Hagness at al.** [36 - 38], and **Fear at al** [29]. The confocal microwave imaging (CMI) technique uses backscattered data gathered by antenna(s) placed at different locations, and an UWB pulse is illuminated as an excitation signal at the transmitting antenna. A two dimensional imaging algorithm which utilizes planar systems as shown in Figure 3-7 was put forward and examined for MRI-based simulation data [8].

In [29] a cylindrical CMI system shown in Figure 3-8 is presented and tested with simulation data. It was observed and verified using three dimensional simulations, simulating breast models that the planar and the cylindrical system has the same performance [39]. Experimental setups and results have also been performed to validate and support the simulation results [40]. For a Confocal Algorithm to be applied on the received signal, first the area of the breast region under consideration is divided in a grid like structure known as focal points.

The distance from the antenna to the focal point is calculated and then these distances are used to find out the time delays. These time delays are used to get the signal values from the received signal to generate the intensity values. These intensities are then mapped and an image is generated to identify the tumor location. Compared to microwave imaging tomography, Confocal Microwave Imaging (CMI) focuses on backscattered signals to form images that indicate reflection of high intensity regions. Tumor produces larger microwave scattering in contrast to the breast tissue. CMI has potential to detect millimeter sized tumors [8].

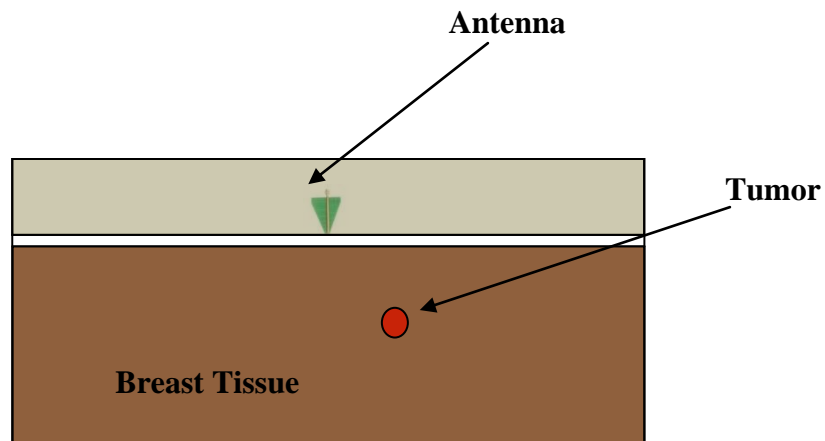


Figure 3-7: Planar Configuration

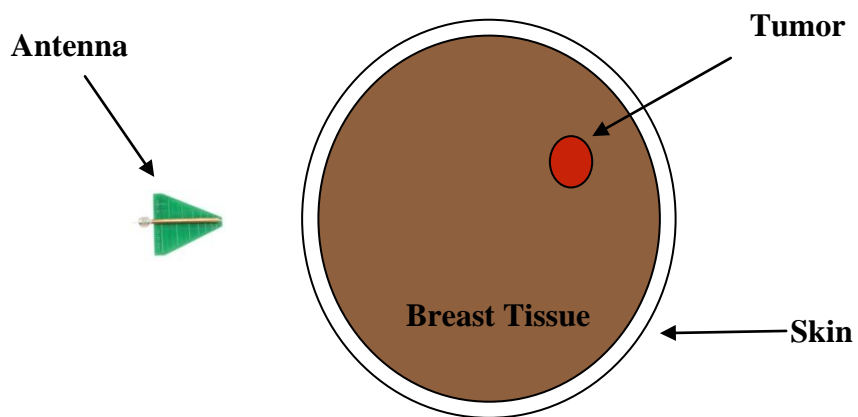


Figure 3-8: Cylindrical Configuration

In order to analyze the effectiveness of the confocal microwave imaging algorithm, an experimental setup is performed and the results are analyzed and discussed in chapter 4.

3.4 Assessment of Microwave Imaging Techniques & Methodology

Microwave breast cancer detection has been developed as an effective and cheaper alternative tool for early detection and diagnoses of breast cancer due to the limitations of the current screening techniques discussed in chapter 2.

Over decades a number of research groups have been proposing microwave imaging as the imaging method for early breast cancer detection and diagnoses [13 - 14, 28, 31]. In comparison with the three microwave imaging techniques passive, hybrid and active as discussed in section 3.1, passive microwave imaging uses temperature difference to detect the location of cancerous tissue in the breast. The main challenge to this method is to detect a very low level power radiated by tumours, which raises technical problems. The other difficulty concerns the estimation of the temperature distribution inside the body. The single frequency radiometry enables measurement of average temperature of a certain area. Therefore, it is hard to distinguish between a cool target close to the skin and a hot target located deep in the breast [46].

On the other hand hybrid microwave imaging uses microwave pulses for imaging whose power is from one to several tens of kilo-watts (Zhurbenko, 2011, p. 95) [46], which is much higher than used by other microwave imaging systems. The inhomogeneity (asymmetric nature) of breast is a major challenge being faced by this technique since the microwave energy illuminated on the breast surface results in a non-uniform response being received that requires complicated algorithms to generate the image. In the hybrid technique, the tissues are heated by the microwave energy, and it is required that the tissues are heated uniformly otherwise the signals will be induced by the non-uniform energy distribution that results in images which are difficult to interpret.

In this technique the breast skin, breast tissues, chest wall, and the tumour absorb microwave energy and convert it to heat energy. This heat energy collected at the receiver is called the thermal acoustic signals. Hence the measured thermal acoustic signal includes responses from the tumour, as well as from other healthy breast tissues.

Due to the high conductivity of the skin the signals generated by the skin are much stronger than that of the small tumours. The high signal strength received by the acoustic sensors (the sensors used in this technique for measuring data) is also due to the fact that the sensors are placed close to the skin [46]. Because of the inhomogeneous nature of the breast, the speed of the acoustic signal received is non-uniform, and therefore causing a problem in accurately determining the time of the acoustic pulse generated at a particular location. All these factors make it difficult to approximate the location of tumour in the breast.

As compared to the passive and hybrid microwave imaging, Active Microwave imaging offers the potential for low cost scanners, non-invasive, harmless and within non-ionizing frequency range because microwaves have the ability to penetrate inside dielectric materials and interact with their inner structure which makes them an excellent candidate for non-invasive and non-ionizing inspection of dielectric media and tumors. This technique is one of the most challenging and attractive application which is divided into micro-wave tomography and radar-based microwave imaging. Both methods depend on a difference in the electrical properties of normal and malignant breast tissues.

Microwave tomography also known as inverse scattering technique illuminates the breast with a narrowband signal and the collected (backscatter) signal is used in a sophisticated algorithm which reconstructs the dielectric (permittivity and conductivity) properties of the breast. The inverse scattering is a non-linear and complex problem which brings lot of challenge to this technique. Its solution relies on the efficiency of the iterative algorithm optimization to reduce the difference between the collected signals to that of the numerical model (simulation) [9]. There are several research groups working on this approach in particular Dartmouth College in USA who so far have reported a clinical prototype and initial clinical testing results in [32].

Unlike the previous approach UWB (Ultra Wide Band) radar based microwave imaging do not attempt to reconstruct the dielectric properties of breast but rather only tries to detect and localize the presence of strong scatter (cancerous tissue). Therefore this approach is less computational complex than microwave tomography. On it the breast is illuminated with a short UWB microwave pulse at different antenna locations and the received backscatter signal is processed to form an image of the tumor. Radar-based imaging systems include microwave imaging via space time

(MIST) beam forming and tissue sensing adaptive radar (TSAR). In TSAR the patient lies in prone position and the breast is illuminated with UWB radar waves with a single antenna in circular configuration, whereas in MIST the patient lies in both prone and supine position and the breast is illuminated with UWB radar waves with an array of antennas in circular and planar configuration respectively as discussed in section 3.3.1 and 3.3.2.

UWB Microwave Radar Imaging is a promising method that has the potential to detect early stage millimeter sized tumors. The advantages of this technology is UWB covers a band of frequencies, such that, low frequencies are needed to ensure a good penetration depth (beneficial for detecting tumors at deeper locations), while high frequencies are necessary to obtain a good spatial resolution (advantage for detecting tumors near the skin) [41]. In addition, it has no breast compression and ionizing radiation making it far less invasive than X-Ray Mammography. Finally, microwave imaging uses very low power so health risks are less of an issue than with previous screening techniques.

One of the most popular algorithms on this approach is the mono-static delay-and-sum beam-forming or confocal microwave imaging algorithm that divides the breast region into fine grid or pixel (focal) points (as in Figure 3-9). The distance between antenna positions and pixel points is calculated and converted to propagation time delay based on the average wave speed. By adding and squaring the delay versions of all the received signals the intensity associated with the pixel (focal) points is evaluated to create an image.

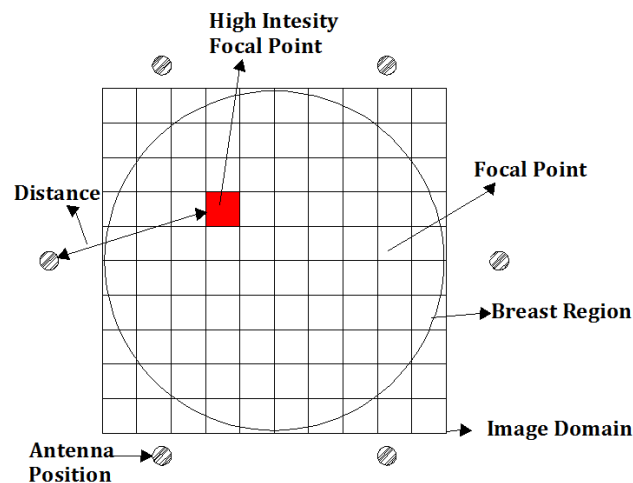


Figure 3-9 A representation of mono-static confocal imaging algorithm

UWB radar based microwave imaging is currently one of the most used research technique on microwave imaging for breast cancer detection.

In correlation with the previous screening methods i.e. MRI, X-ray mammography and Ultrasound extensive research adopting microwave imaging has been conducted for the purpose of breast cancer detection [3, 7 – 8, 41, 44 - 45]. The high contrast in the dielectric properties between normal and cancerous breast tissues is the appealing factor for tumour detection with microwave imaging and non-invasive testing techniques. The interaction of electromagnetic waves, at microwave frequencies, with multilayered dielectric media is fundamental for any microwave screening or testing application. Also, detection of tumors in their early stages is a very important step in order for the patient to be treated without any surgical operation or medical action that would negatively affect the patient's life.

Research on early tumour detection using microwave imaging techniques has been possible due to the work of many researchers using different methods and algorithms to determine the location of tumour with significant results. The research at Durham University focuses on experimental analysis of breast tumour detection using different materials are used as tumour to study the response of tumour with the variation of antenna distance using Confocal Microwave Imaging algorithm discussed in chapter 4. The purpose of using different materials as tumour is to determine the effectiveness of confocal algorithm by creating an image of the tumour response for patients having different dielectric permittivity(s) of tumour.

4 EXPERIMENTAL ANALYSIS ON EFFECTIVENESS OF CMI ALGORITHM

4.1 Overview

The experimental set up was arranged to analyze the confocal algorithm's feasibility using different materials as tumour, to study the response of tumour with the variation in antenna distance. In the experiment, Vector Network Analyzer (VNA) E5071 Agilent Technology was used for measurements. A **Network Analyzer** is an instrument that measures the scattering parameters (backscatter response) of electrical networks and is widely used for RF design applications. Before the measurements were taken through the vector network analyzer, calibration was performed using the Calibration Kit, which is used to calibrate the SMA Cable that was connected to the antenna to determine the scattering parameters relative to the antenna only. After the calibration process is completed, the VNA is ready to take the measurements. The scattering parameters were obtained using the VNA with a directive antenna (log periodic antenna) connected via a 50 ohm SMA Cable, providing the start and stop frequency of 2.1 and 8.5 GHz respectively.

In order to analyze the feasibility of confocal algorithm we start with a simple experimental setup due to the lack of availability of materials with permittivity of normal breast tissue, therefore we simulate the normal tissue as air. The tumor is simulated with different materials of 10-20 mm diameter each. Log periodic antenna of 2 to 11 GHz is used to record the measurements. XY-Positioner is used in order to position and support the antenna in a grid of 100 mm by 100 mm. Table 4-1 lists the materials used with their respective permittivity [42].

Table 4-1 – Permittivity of Materials Used in the Experiment [42]

Materials	Water	Glass	Plastic	Silicon	Dry Wood	Rubber	PVC	Copper
Permittivity	4-88	3.7-10	1.1-3.2	11.0-12.0	2-6	2.7-2.9	2.8-3.4	18.1

The breast phantom is illuminated by the antenna and the scattering parameters are recorded in the specified swept frequency range (2.1 to 8.5 GHz). The number of points for the VNA measurement is the total number of samples collected per sweep. It can be a set to any number from 2 to 1601 for each channel independently. To obtain a higher trace resolution in our experimental setup, the data is recorded at 1601 frequency points and for each frequency the final scattering parameter is obtained by averaging 16 acquisitions. Averaging is effective in reducing random noise in performing measurements. The X-Y Positioner moves the antenna to 36 different and the measurement is performed at each position.

4.1.1 Explanation of Experimental Setup

This section discusses the experimental setup in detail which was used to analyze the effectiveness of confocal microwave imaging algorithm for different materials as tumor. The current technique for radar based microwave imaging consist of transmitting short pulse into the breast phantom and processing the collected reflections, as previously discussed in chapter 3. Due to the difficulty on hardware for producing ultra wideband pulses and fulfill the requirements for high dynamic range and measurement accuracy, all the experimental set up for pulse based method rely on frequency domain measurements of the scattering network parameters performed with a vector network analyzer (VNA).

The pulse time domain characteristic is synthesized, using MATLAB software, through the inverse Fast Fourier Transform of the scattering parameters from the VNA. The breast phantoms in our experiment are built of liquid and solid materials as in Table 1. The vector network analyzer as we said serves as transmitter and receiver. The personal computer (PC) is used for signal processing and also controls the VNA and antenna positions.

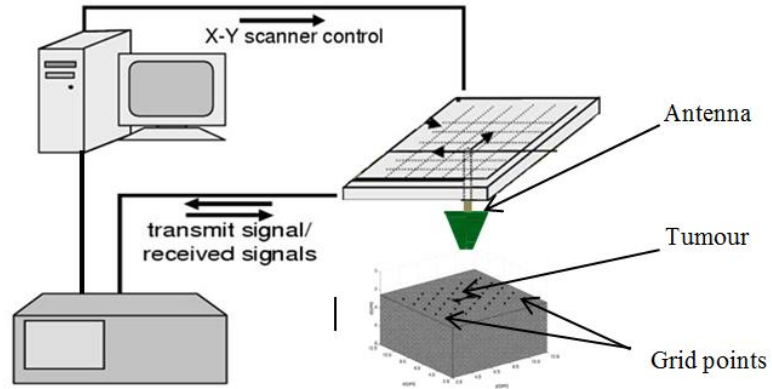


Figure 4-1: Modified Experimental setup as in [38]

Figure 4-1 shows the experimental setup which was used to investigate the effectiveness of Confocal Microwave Imaging algorithm for different materials (water, glass, plastic, silicon, wood, rubber, PVC and copper) as tumor. Before performing the experiment the apparatus was set up in an RF Anechoic Chamber at Durham University.

RF Anechoic chamber is covered with radiation absorbent material which are designed and shaped to absorb electromagnetic radiation (also known as non-ionizing radiation) as much as possible from various incident directions. This chamber was used in our experiment to minimize the unwanted noise and reflections from the surrounding that affects the location and existence of the tumor to minimize the false positive rate (presence and/or location of tumor detected in healthy breast) and false negative rate (presence and/or location of tumor not detected in unhealthy breast). The main apparatus used in our experiment is as follows:

➤ **Vector Network Analyzer (VNA)**

A network analyzer was used as “sweep generator” to provide an ultra-wideband signal. We do have available a 4-port network analyzer (VNA) the Agilent “E5071A” which operates within 300 KHz – 8.5GHz frequency range, which is able to perform 4 channels (antennas) measurements simultaneously. A further 9-port multipoint extension set the Agilent “E5092A” is

also available in our lab. In our experiment we used single port analysis using mono-static antenna configuration.

➤ **X-Y Probe**

X-Y probe was assembled and built together with its control parts in University of Durham by another researcher of our group. The probe is used to accurately move the antenna into predefined positions in a grid of 100mm by 100mm. The program to control the X-Y probe was written in “Mach3” motion control software package.

➤ **Personal Computer (PC)**

Apart for the processing of measurement data, which was done through MATLAB software, the PC played a major role in the synchronization and control of the devices on the experimental set up. The mode of operation to be controlled by the PC is as follows:

1. The PC sends a signal to X-Y probe to moves the antenna into a predefined position, once completed it reports back to the PC
2. PC then sends a start measurement signal to VNA and waits for the finish sweep report from the VNA.
3. The measurement data for the corresponding position is saved on the PC.
4. Cycle back to step (1) – (3) until the measurement in the predefined position has been completed.

➤ **Breast Phantom**

A breast phantom that mimics the physical and electric properties of the breast tissue is an important component in experiments as it aids on testing and development of the microwave imaging technique. In our experiment the breast phantom is simulated by using air as a normal tissue and different materials as tumor.

➤ **Antenna**

Antenna plays a crucial role in any wireless system. It converts the electric signal present on the transmission line or waveguide into radiating electromagnetic wave travelling in free space and vice - versa. For UWB radar based microwave imaging the antenna has to efficiently operate on wide bandwidth to produce as minimum as possible distortion and dispersion on transmitted or received signal, and be of small size and low cost. On this application an antenna with directive pattern is highly desirable. We therefore used a log-periodic antenna in mono-static configuration within 2.1 – 8.5GHz frequency range.

The measurement procedure is as follows;

- a) The log-periodic antenna is sequentially repositioned in the horizontal plane using a computer-controlled mechanical –scanner (X-Y Positioner) to synthesize a 2-D antenna array placed above the breast phantom.
- b) At each X-Y antenna position, the PC triggers the Vector Network Analyzer and 1601 measurement points for reflection coefficient (scattering parameters) over the frequency band 2.1 to 8.5GHz are performed.
- c) Having obtained the frequency domain data for the particular antenna position, the results are stored in the PC and the probe is moved to a new position and the measurement procedure is repeated.
- d) The obtained data is then processed by the PC to create an image using Confocal Microwave Imaging Algorithm discussed in section 4.2.

4.2 Implementation of Con-Focal Algorithm

4.2.1 Process Flow Diagram of Algorithm

This section will explain the implementation of Confocal Algorithm. Figure 4-2 shows the process flow used to create an image of the tumor.

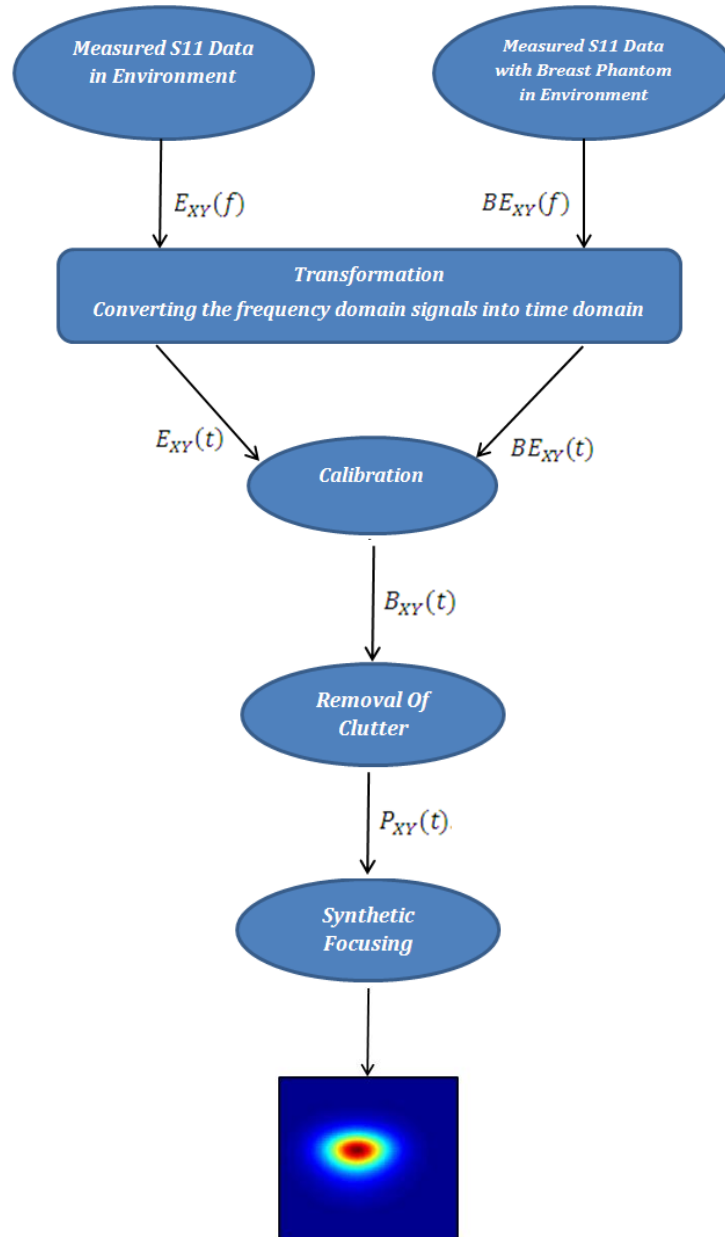


Figure 4-2: Process Flow Diagram of Confocal Algorithm

As discussed in section 4.1.1, to create the image of tumor confocal algorithm is used. Two sets of frequency domain data are obtained from the VNA at antenna position(s) XY ;

- i. In the **Environment** $E_{XY}(f)$ (involves reflections from different sources which are used for experimental work, i.e. VNA, PC, X-Y Positioner, surroundings etc.)
- ii. In the presence of **Breast phantom** $BE_{XY}(f)$ (different materials simulated as tumor in environment)

The frequency domain measurements (i) and (ii) at antenna positions XY are transformed into time domain by Inverse Fast Fourier Transform (IFFT). The obtained time domain signals $E_{XY}(t)$ & $BE_{XY}(t)$ are then calibrated in the calibration process which involves subtracting the response of the Environment $E_{XY}(t)$ with that of the Breast phantom in environment $BE_{XY}(t)$ to remove the Environment signal(s) $E_{XY}(t)$ so that we can get approximate Breast Phantom signal(s) $B_{XY}(t)$.

The Breast Phantom signal(s) $B_{XY}(t)$ still contains reflection due to the antenna. To delete, or reduce the reflections due to antenna, the Breast Phantom signal(s) $B_{XY}(t)$ are averaged and the averaged signal is then subtracted to each of the Breast Phantom signal(s) $B_{XY}(t)$. The signal(s) obtained after subtraction are called the Processed signal(s) $P_{XY}(t)$. The Processed signal(s) $P_{XY}(t)$ are synthetically focused to generate the approximate image of Breast Phantom containing tumor. The process flow in Figure 4-2 is further explained in section 4.2.2.

4.2.2 Explanation of the Process Flow

Frequency domain data (scattering parameters) is obtained from VNA when antenna is exposed to the environment and when antenna is exposed to the breast phantom in environment. The frequency domain data $E_{XY}(f)$ & $BE_{XY}(f)$ are then transformed to time domain for further processing. The details of each process are discussed below;

i. Transformation

The antenna is excited with a sweep signal generated by the Vector Network Analyzer (VNA), at 36 different positions in a grid (6 x 6) of covered area 100 mm by 100 mm as shown in Figure 4-3, at different height (1cm and 3cm) from tumor.

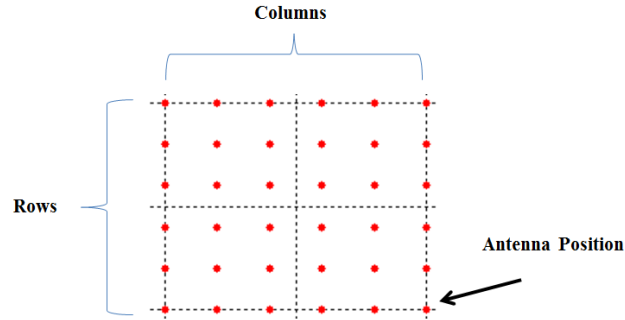


Figure 4-3: Antenna positions covered in an area of 100mm by 100mm

The frequency domain data (Environment $E_{XY}(f)$ and Breast Phantom in Environment $BE_{XY}(f)$) obtained from the VNA is first windowed using the Hamming window. A Hamming window is applied to the signal(s) to reduce the level of side lobes. The obtained signal is then transformed into time domain by taking the Inverse Fast Fourier Transform (IFFT) of the signal(s).

$$E_{XY}(f)_{windowed} = E_{XY}(f) * w$$

$$BE_{XY}(f)_{windowed} = BE_{XY}(f) * w$$

$$E_{XY}(t) = ifft(E_{XY}(f)_{windowed})$$

$$BE_{XY}(t) = ifft(BE_{XY}(f)_{windowed})$$

Where;

w is the Hamming window signal;

XY are the antenna positions defined by row X and column Y in a grid. The grid is represented as a matrix of 6 rows and 6 columns. For 36 antenna positions, the matrix is as follows;

$$\begin{bmatrix} (1,1) & (1,2) & (1,3) & (1,4) & (1,5) & (1,6) \\ (2,1) & (2,2) & (2,3) & (2,4) & (2,5) & (2,6) \\ (3,1) & (3,2) & (3,3) & (3,4) & (3,5) & (3,6) \\ (4,1) & (4,2) & (4,3) & (4,4) & (4,5) & (4,6) \\ (5,1) & (5,2) & (5,3) & (5,4) & (5,5) & (5,6) \\ (6,1) & (6,2) & (6,3) & (6,4) & (6,5) & (6,6) \end{bmatrix}$$

$E_{XY}(t)$ and $BE_{XY}(t)$ are the time domain signals for Environment and Breast phantom in environment at time t respectively. Therefore for 36 antenna positions $E_{XY}(t)$ and $BE_{XY}(t)$ can be represented as;

$$\begin{bmatrix} E_{11}(t) & E_{12}(t) & E_{13}(t) & E_{14}(t) & E_{15}(t) & E_{16}(t) \\ E_{21}(t) & E_{22}(t) & E_{23}(t) & E_{24}(t) & E_{25}(t) & E_{26}(t) \\ E_{31}(t) & E_{32}(t) & E_{33}(t) & E_{34}(t) & E_{35}(t) & E_{36}(t) \\ E_{41}(t) & E_{42}(t) & E_{43}(t) & E_{44}(t) & E_{45}(t) & E_{46}(t) \\ E_{51}(t) & E_{52}(t) & E_{53}(t) & E_{54}(t) & E_{55}(t) & E_{56}(t) \\ E_{61}(t) & E_{62}(t) & E_{63}(t) & E_{64}(t) & E_{65}(t) & E_{66}(t) \end{bmatrix} \quad \begin{bmatrix} BE_{11}(t) & BE_{12}(t) & BE_{13}(t) & BE_{14}(t) & BE_{15}(t) & BE_{16}(t) \\ BE_{21}(t) & BE_{22}(t) & BE_{23}(t) & BE_{24}(t) & BE_{25}(t) & BE_{26}(t) \\ BE_{31}(t) & BE_{32}(t) & BE_{33}(t) & BE_{34}(t) & BE_{35}(t) & BE_{36}(t) \\ BE_{41}(t) & BE_{42}(t) & BE_{43}(t) & BE_{44}(t) & BE_{45}(t) & BE_{46}(t) \\ BE_{51}(t) & BE_{52}(t) & BE_{53}(t) & BE_{54}(t) & BE_{55}(t) & BE_{56}(t) \\ BE_{61}(t) & BE_{62}(t) & BE_{63}(t) & BE_{64}(t) & BE_{65}(t) & BE_{66}(t) \end{bmatrix}$$

ii. Calibration

The calibration process involves subtracting the response of the Environment $E_{XY}(t)$ with that of the Breast phantom in environment $BE_{XY}(t)$ to remove the Environment signal(s) $E_{XY}(t)$ so that we can get approximate Breast Phantom signal(s) $B_{XY}(t)$. This subtraction generates a higher peak at the location of the tumor by reducing the environment response from the target signal. The subtracted signal contains the Breast phantom signal.

$$B_{XY}(t) = BE_{XY}(t) - E_{XY}(t)$$

Where $B_{XY}(t)$ is the Breast phantom signal at time t for 36 antenna positions;

$$\begin{bmatrix} B_{11}(t) & B_{12}(t) & B_{13}(t) & B_{14}(t) & B_{15}(t) & B_{16}(t) \\ B_{21}(t) & B_{22}(t) & B_{23}(t) & B_{24}(t) & B_{25}(t) & B_{26}(t) \\ B_{31}(t) & B_{32}(t) & B_{33}(t) & B_{34}(t) & B_{35}(t) & B_{36}(t) \\ B_{41}(t) & B_{42}(t) & B_{43}(t) & B_{44}(t) & B_{45}(t) & B_{46}(t) \\ B_{51}(t) & B_{52}(t) & B_{53}(t) & B_{54}(t) & B_{55}(t) & B_{56}(t) \\ B_{61}(t) & B_{62}(t) & B_{63}(t) & B_{64}(t) & B_{65}(t) & B_{66}(t) \end{bmatrix}$$

iii. Clutter Removal

The Breast phantom signals $B_{XY}(t)$ at location X and Y , still contains reflections dominated due to the antenna and the environment. In order to reduce the reflections due to antenna and environment, the Breast Phantom signal(s) $B_{XY}(t)$ are first averaged. The averaging is done by adding the Breast Phantom signal(s) $B_{XY}(t)$ in a given row of grid (6 x 6), and dividing it with the total number of antenna positions in that row N (total of 6 antenna positions in a given row for our experiment). These signals are known as the averaged signals $A_X(t)$.

$$A_X(t) = \frac{\sum_{Y=1}^N B_{XY}(t)}{N}$$

Where N is the total number of antenna positions in a row;

$A_X(t)$ is the averaged signal at row X at time t . For 6 rows the signals $A_X(t)$ can be represented as;

$$\begin{bmatrix} A_1(t) \\ A_2(t) \\ A_3(t) \\ A_4(t) \\ A_5(t) \\ A_6(t) \end{bmatrix}$$

The averaged signals $A_X(t)$ are then subtracted to each of the Breast Phantom signal(s) $B_{XY}(t)$. The subtracted signals are known as the Processed Signal(s) $P_{XY}(t)$.

$$P_{XY}(t) = B_{XY}(t) - A_X(t)$$

$P_{XY}(t)$ is the processed signal(s) at location XY at time t . For 36 antenna positions the signals $P_{XY}(t)$ can be represented as;

$$\begin{bmatrix} P_{11}(t) & P_{12}(t) & P_{13}(t) & P_{14}(t) & P_{15}(t) & P_{16}(t) \\ P_{21}(t) & P_{22}(t) & P_{23}(t) & P_{24}(t) & P_{25}(t) & P_{26}(t) \\ P_{31}(t) & P_{32}(t) & P_{33}(t) & P_{34}(t) & P_{35}(t) & P_{36}(t) \\ P_{41}(t) & P_{42}(t) & P_{43}(t) & P_{44}(t) & P_{45}(t) & P_{46}(t) \\ P_{51}(t) & P_{52}(t) & P_{53}(t) & P_{54}(t) & P_{55}(t) & P_{56}(t) \\ P_{61}(t) & P_{62}(t) & P_{63}(t) & P_{64}(t) & P_{65}(t) & P_{66}(t) \end{bmatrix}$$

The processed signals(s) $P_{XY}(t)$ will then be used to generate the intensity values at time t for the formation of image. For generating the intensity values, apart from the processed signals we also need the round trip time. For getting the round trip time we need to perform synthetic focusing which is discussed in detail.

iv. Synthetic Focusing

The synthetic focusing is performed by computing the round trip time. In order to evaluate the round trip time following steps were performed;

- a) Generate pixel points.
- b) Evaluate the distance from each antenna position to each pixel point
- c) Generate the round trip time.

a) Generate Pixel points

To generate the pixel points $F(x_i, y_j)$ at coordinates x_i and y_j , we considered an area of (300 mm by 300 mm) rather considering the area covered by the antenna positions (100mm by 100mm) for better resolution of the image. Figure 4-4 shows the pixel points (represented by blue dots) locations in a covered area of 300mm by 300mm.

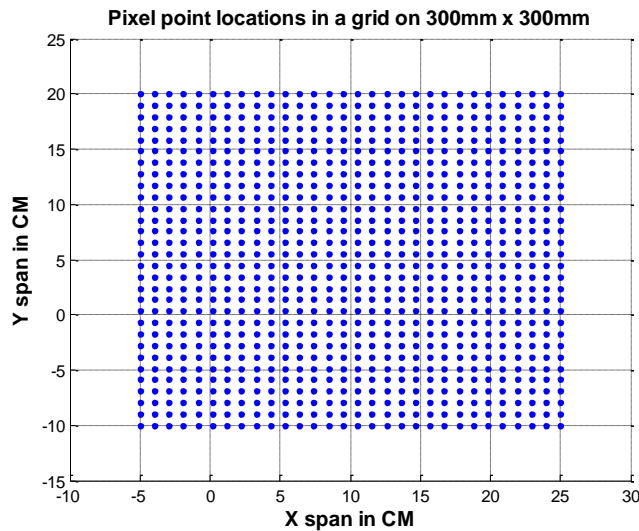


Figure 4-4: Pixel point locations for Synthetic focusing to find time values

b) Evaluate the distance(s) of each antenna location to the pixel point(s)

The distance(s) of each antenna position XY to the pixel (x_i, y_j) were evaluated using the following equation;

$$D_{XY}(x_i, y_j) = 2\sqrt{(X - x_i)^2 + (Y - y_j)^2 + h^2}$$

Where;

h is the height of the antenna (1cm or 3cm) from the tumor;

x_i and y_j define the coordinates of the pixel points as shown in Figure 4-4;

The antenna positions are defined by X and Y ;

$D_{XY}(x_i, y_j)$ is the round trip distance for antenna position XY to the pixel (x_i, y_j) .

In the experiment we have used single antenna as transmitter and receiver. Therefore the distance covered by the transmitter to each pixel point and by the receiver to each pixel point will be same. Therefore we multiply the distance by 2. Figure 4-5 shows the method for finding the round trip distance from each antenna position to each pixel point.

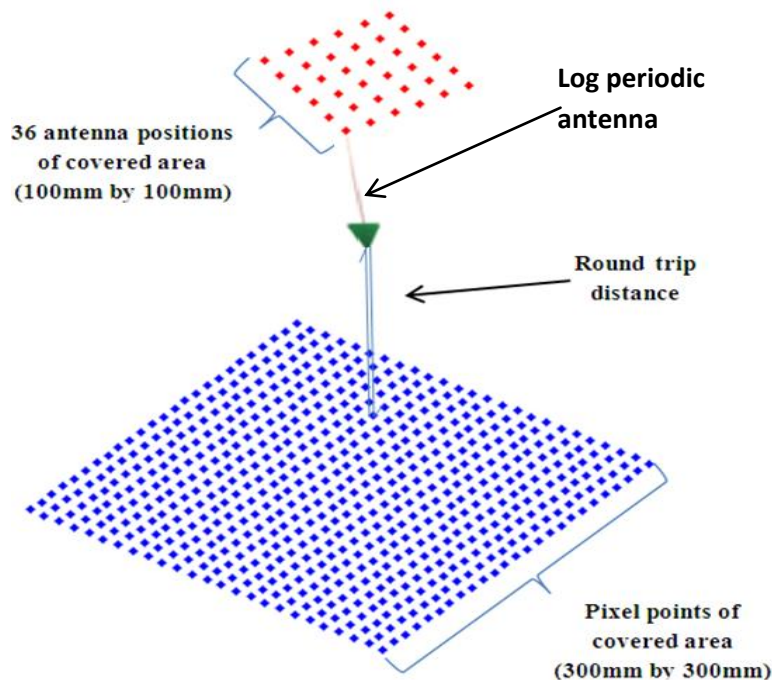


Figure 4-5: Representation of finding the round trip distance of each Antenna position to the Pixel points

c) Generate the round trip time

The round trip time is finally calculated for antenna position XY at pixel (x_i, y_j) by the following equation;

$$t_{XY}(x_i, y_j) = \frac{D_{XY}(x_i, y_j)}{c/\sqrt{\epsilon_r}}$$

Where c is the speed of light in cm/s ;

ϵ_r is the permittivity of the medium (air $\epsilon_r = 1$ for our experiment)

$t_{XY}(x_i, y_j)$ is the round trip time from antenna position XY to pixel (x_i, y_j)

v. Image

As discussed before to generate the intensity values to form the image, apart from the processed signal $P_{XY}(t)$, time values are also needed. After calculating the time values $t_{XY}(x_i, y_j)$ for each antenna position XY at pixel (x_i, y_j) , the Intensity values are generated for each pixel points by evaluating the signal value of the processed signal $P_{XY}(t)$ at time $t_{XY}(x_i, y_j)$. Mathematically the intensity values at pixel (x_i, y_j) is represented as

$$I(x_i, y_j) = \left[\sum_{X=1}^r \sum_{Y=1}^c P_{XY}(t_{XY}(x_i, y_j)) \right]^4 \quad [39]$$

Where;

r is the total number of antenna positions in a row;

c is the total number of antenna positions in a column;

$I(x_i, y_j)$ is the intensity value at pixel point (x_i, y_j)

The reason behind taking the 4th power instead that the second power as in [13] has been done after several tests by research group at the University of Calgary [39] since they observed that the 4th power proved to suppress the clutter but affected the size of tumor whereas in [13] the 2nd power did not suppress the clutter as compared to the 4th power and the size of the tumor was also not affected.

The experimental analysis was also performed at the University of Durham [43] to compare the effects using different approximations (2nd power and 4th power) to suppress the clutter. Figure 4-6(a) and 4-6(b) shows the experimental results of the two approximations where we observed that the clutter is suppressed using the 4th power in Figure 4-6(b) and hence 4th power is used to investigate the effectiveness of Confocal Microwave Imaging Algorithm.

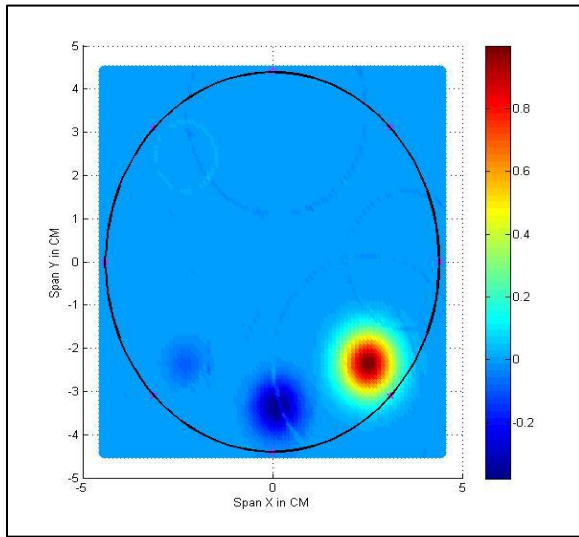


Figure 4-6(a) Image using 2nd Power

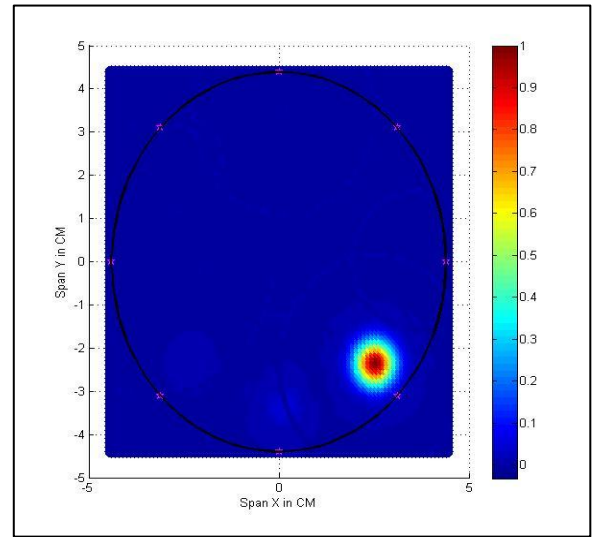


Figure 4-6(b) Image using 4th Power.

5 DISCUSSIONS & EXPERIMENTAL RESULTS

In this chapter the result and work undertaken for this project has been analyzed and interpreted. The assumptions and the outcomes of the results have been critically evaluated using other published works. The discussions of the work involved in this project can be divided into three main parts:

1. Experimental Measurements.
2. Confocal Algorithm.
3. Analysis on the results.

Section 5.1 will discuss the measurements performed by using the experimental setup (when the antenna is illuminated in the environment and when the antenna is illuminated to the breast phantom in the environment); Section 5.2 will discuss the confocal algorithm in detail with the steps involved in generating the final results from the measurements obtained by the performed experiment; Section 5.3 will discuss the results in detail to evaluate the effectiveness of using Confocal Microwave Imaging Algorithm for radar based breast cancer detection.

5.1 Experimental Measurements

The Vector Network Analyzer (VNA) model number E5071 was used to measure the backscatter response (scattering parameters) of the antenna when it was illuminated 1) In the environment 2) In the Environment with the presence of Breast phantom (different materials simulated as tumor where air is considered as the normal tissue) as discussed in chapter 4. Figure 5-1 shows the measurements of the backscatter response when the antenna subjected in the environment and Figure 5-2 shows the measurements of the backscatter response when the antenna is subjected in the environment with the presence of breast phantom.

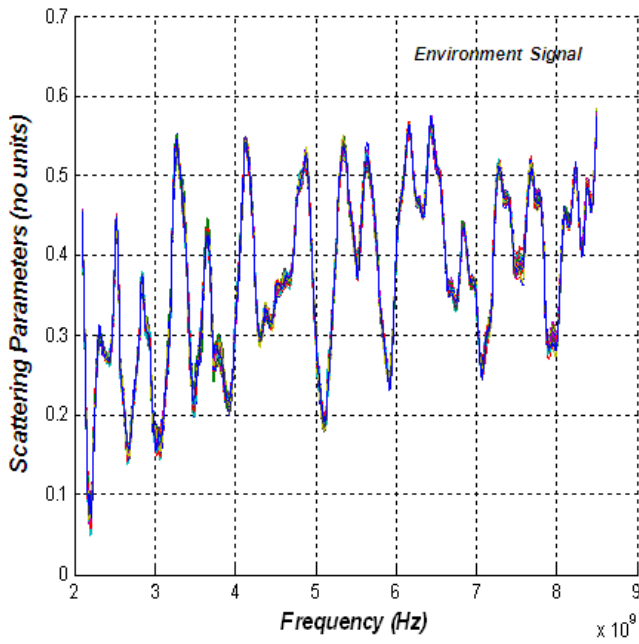


Figure 5-1: Measured scattering parameters in Environment

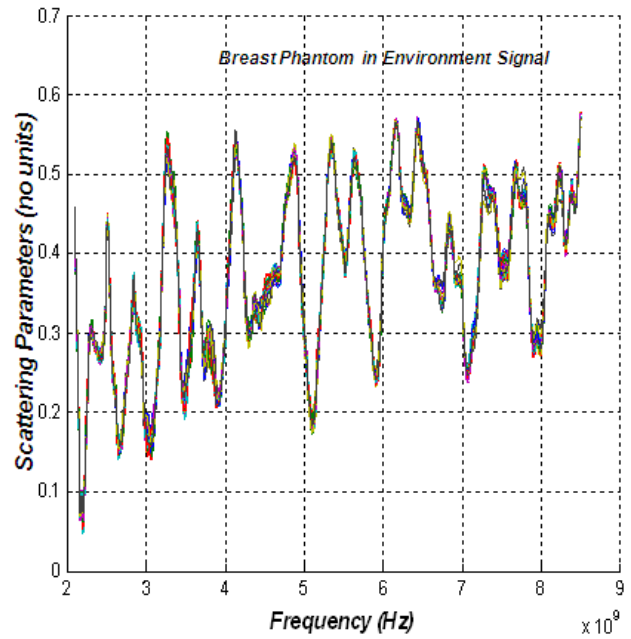
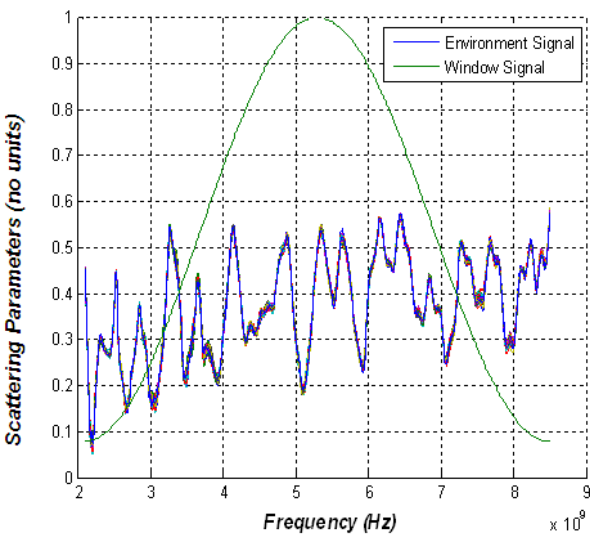
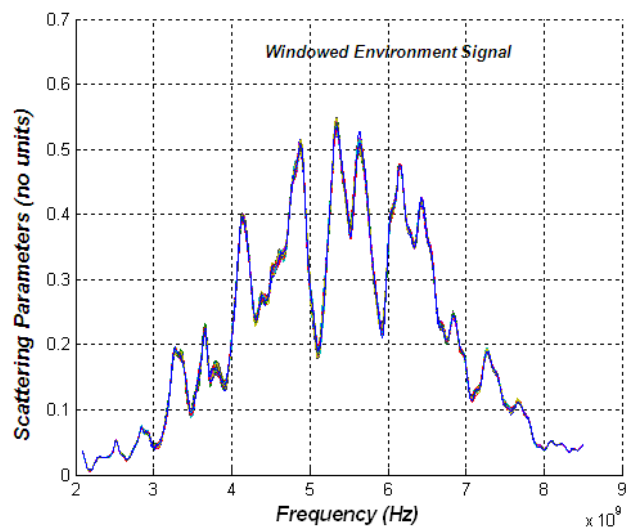


Figure 5-2: Measured scattering parameters in Environment in the presence of Breast Phantom

The measured backscatter data (in the environment and the breast phantom in the environment) obtained from the VNA is then windowed using the Hamming window. A Hamming window is applied to the signal(s) to minimize the level of the side lobes. Figure 5-3(a) and 5-3(b) illustrates the effect of applying the hamming window to the environment signal.



(a)



(b)

Figure 5-3 (a) Illustration of Environment Signal with hamming window (b) Response of Environment Signal after applying hamming window

We have applied the hamming window to the rest of the measured backscatter data which includes the data obtained when antenna is exposed to the breast phantom (with different materials as tumour) in the environment. After applying the hamming window to each signal(s), the resulting signal(s) is transformed into the time domain by taking the Inverse Fast Fourier Transform (IFFT) of the signal(s) for further processing in Confocal Algorithm. Figure 5-4 illustrates the time domain response of the Environment signal by taking the Inverse Fast Fourier Transform.

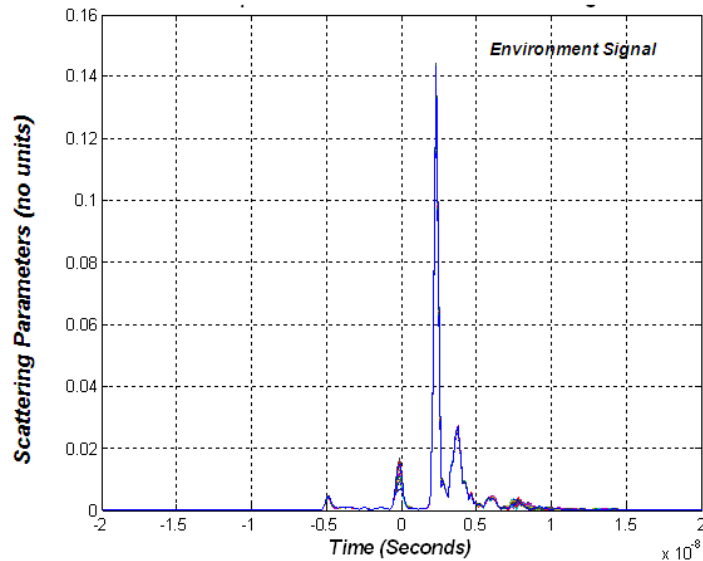


Figure 5-4: Response of Environment Signal after applying Inverse Fast Fourier Transform

We have applied the Inverse Fast Fourier Transform to the rest of the measured backscatter data that includes the data obtained when antenna is exposed to the breast phantom (with different materials as tumour) in the environment. After the time domain data is obtained, it is then applied into the confocal algorithm for generating the results of different materials as tumour.

5.2 Confocal Algorithm

To evaluate the effectiveness of Confocal Microwave Imaging, the algorithm is written in MATLAB to generate the results of different materials used in our experiment as tumour.

After the backscatter signals were transformed into time domain as discussed in section 5.1, confocal algorithm is applied, where first calibration of the signals has been carried and the environment response is removed to get the approximate Breast Phantom Response. Figure 5-5 shows the Breast Phantom response.

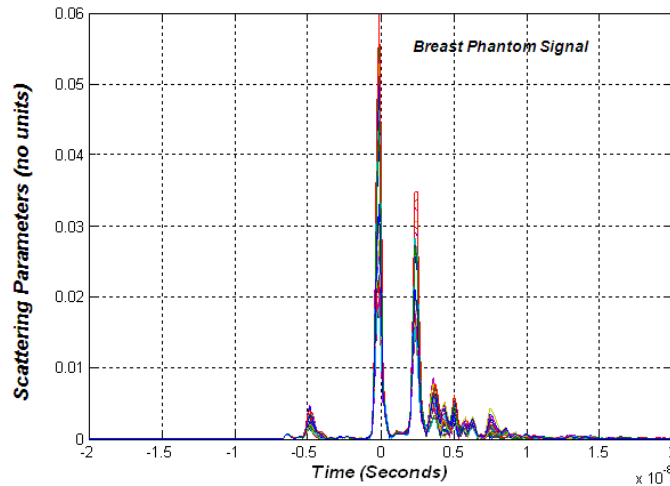


Figure 5-5: Response of Tumor Signal after removing the Antenna Backscatter

After getting the approximate Breast Phantom response, synthetic focusing is performed (which is already explained in detail in section 4.2.2(iv)) to generate the image of Breast phantom containing tumor. Figure 5-6 to Figure 5-12 are the results obtained by the experiment performed which are evaluated using MATLAB. The analysis of the result is discussed in section 5.3 to assess the effectiveness of the confocal microwave imaging algorithm.

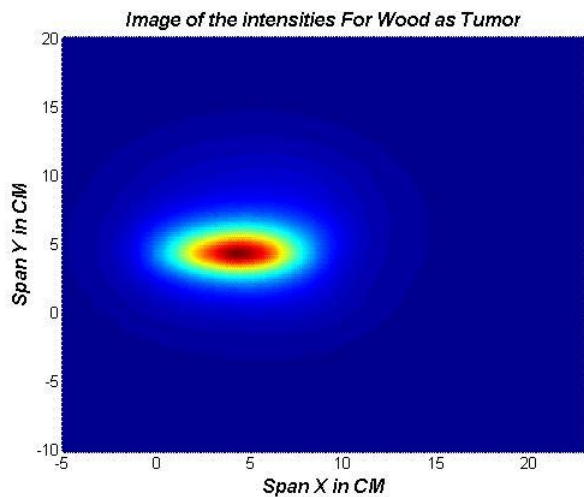


Figure 5-6 (a) 1 cm Distance

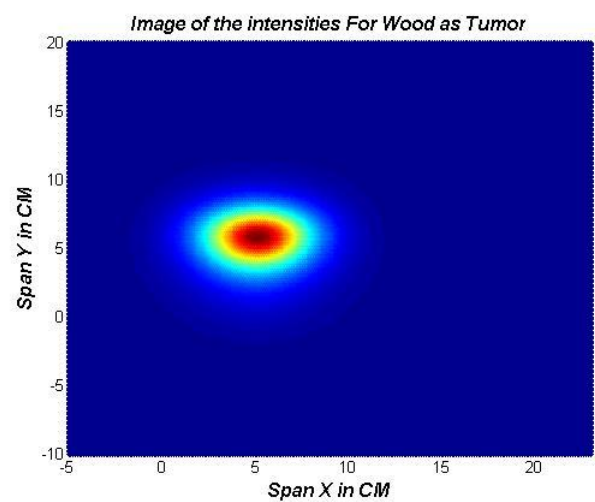


Figure 5-6 (b) 3 cm Distance

Figure 5-6 (a) & (b) shows the Image of the intensity values when the antenna is subjected to the Breast Phantom (environment containing wood as tumor), where Wood is taken as tumor at a depth of 1cm and 3 cm respectively.

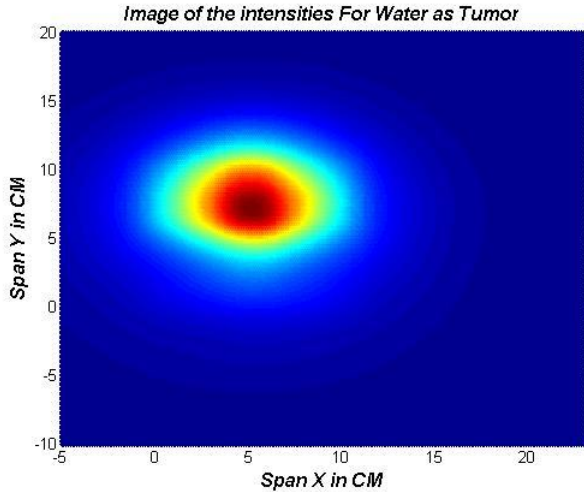


Figure 5-7 (a) 1 cm Distance

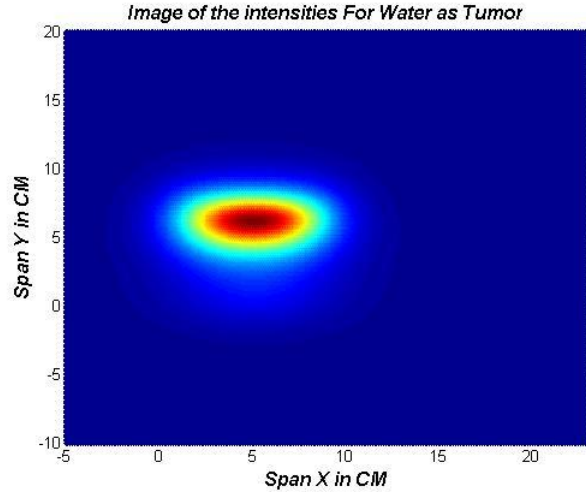


Figure 5-7 (b) 3 cm Distance

Figure 5-7 (a) & (b) shows the Image of the intensity values when the antenna is subjected to the Breast Phantom (environment containing water as tumor), where water is taken as tumor at a depth of 1cm and 3 cm respectively.

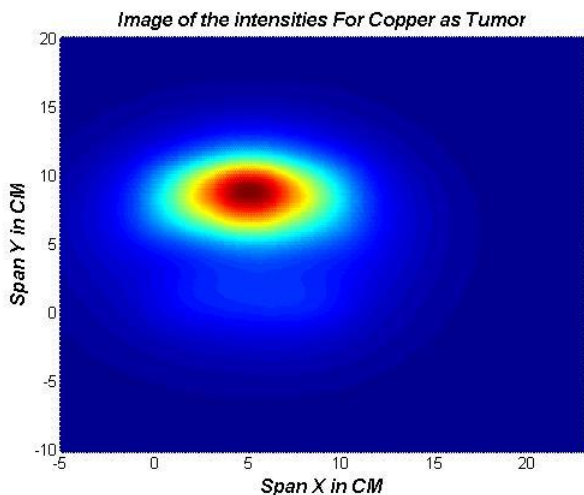


Figure 5-8 (a) 1 cm Distance

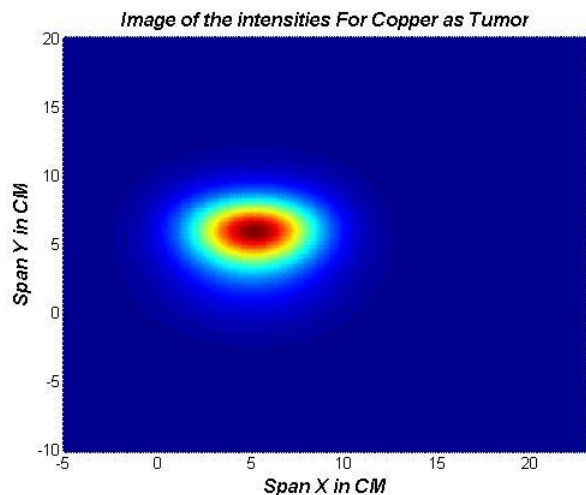


Figure 5-8 (b) 3 cm Distance

Figure 5-8 (a) & (b) shows the Image of the intensity values when the antenna is subjected to the Breast Phantom (environment containing copper as tumor), where copper is taken as tumor at a depth of 1cm and 3 cm respectively.

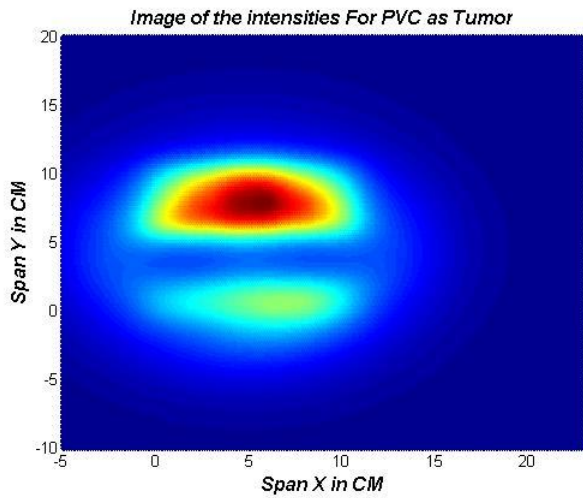


Figure 5-9 (a) 1 cm Distance

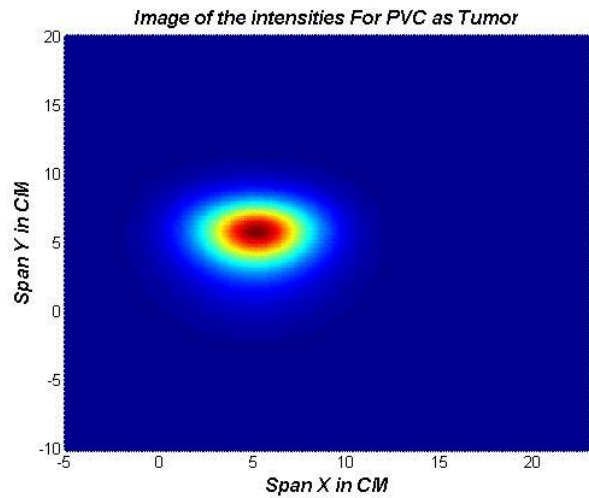


Figure 5-9 (b) 3 cm Distance

Figure 5-9 (a) & (b) shows the Image of the intensity values when the antenna is subjected to the Breast Phantom (environment containing PVC as tumor), where PVC is taken as tumor at a depth of 1cm and 3 cm respectively.

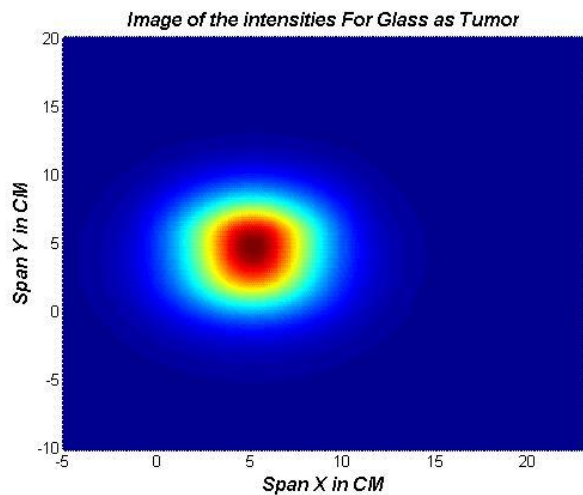


Figure 5-10 (a) 1 cm Distance

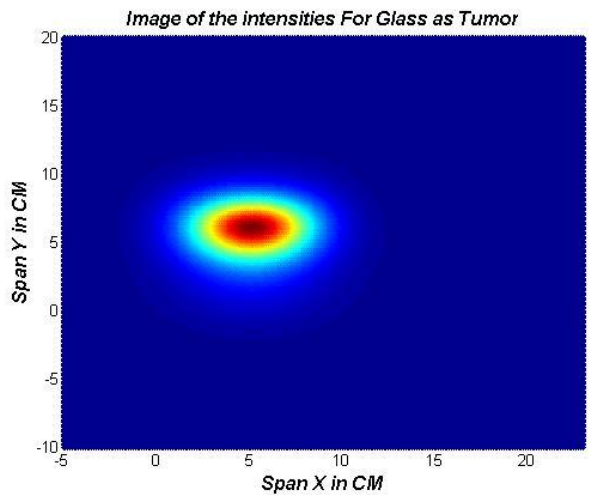


Figure 5-10 (b) 3 cm Distance

Figure 5-10 (a) & (b) shows the Image of the intensity values when the antenna is subjected to the Breast Phantom (environment containing glass as tumor), where glass is taken as tumor at a depth of 1cm and 3 cm respectively.

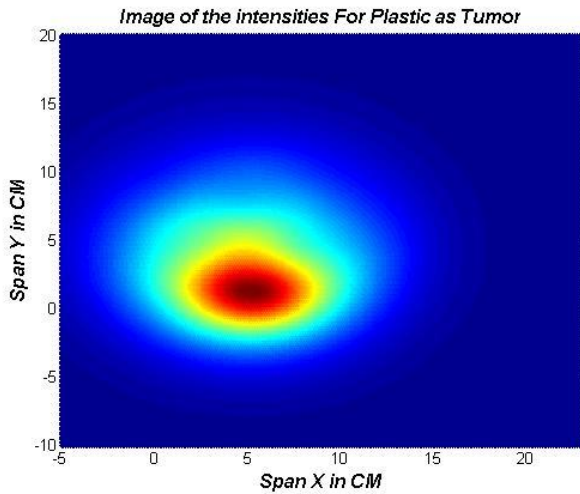


Figure 5-11 (a) 1 cm Distance

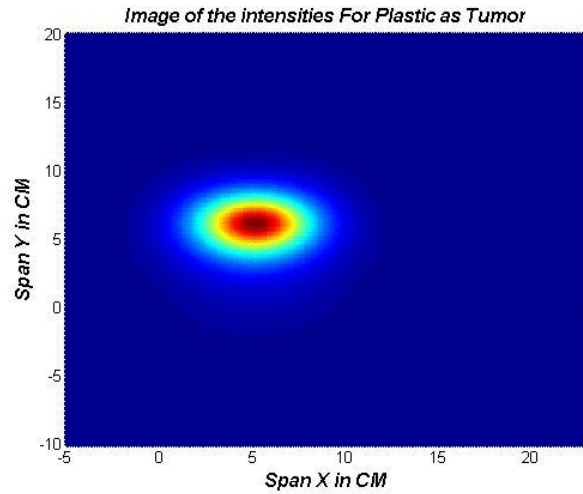


Figure 5-11 (b) 3 cm Distance

Figure 5-11 (a) & (b) shows the Image of the intensity values when the antenna is subjected to the Breast Phantom (environment containing plastic as tumor), where plastic is taken as tumor at a depth of 1cm and 3 cm respectively.

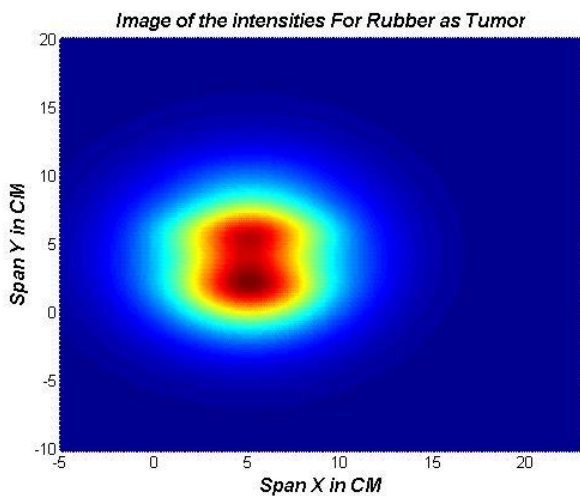


Figure 5-12 (a) 1 cm Distance

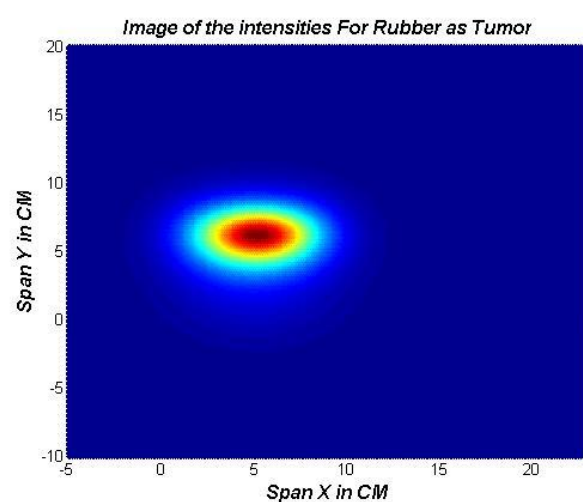


Figure 5-12 (b) 3 cm Distance

Figure 5-12 (a) & (b) shows the Image of the intensity values when the antenna is subjected to the Breast Phantom (environment containing rubber as tumor), where rubber is taken as tumor at a depth of 1cm and 3 cm respectively.

5.3 Analysis on the results

Figures 5-6 to Figure 5-12 shows the responses for all the materials as tumor for antenna distances at 1cm and 3cm. It is noted that the effectiveness of the confocal algorithm signifies the tumour responses for all the materials in Table 1 chapter 4, but the antenna distance from the object indicated that certain materials (PVC, glass, plastic, rubber, wood) tend to generate more scatter in the surrounding.

The significance of the amount of scatter is dependent on the size and the electrical conductivity of the material. Since the materials (PVC, glass, plastic, rubber and wood) are less electrically conductive as compared to water copper, the transmitted signals from the antenna dissipate in the surrounding. As the size of the material increase, larger area is covered and more signal is dissipated in the environment. If the amount of additional scatter is more, then the size of the tumor detected is affected which generates problems in identifying the actual size of tumor.

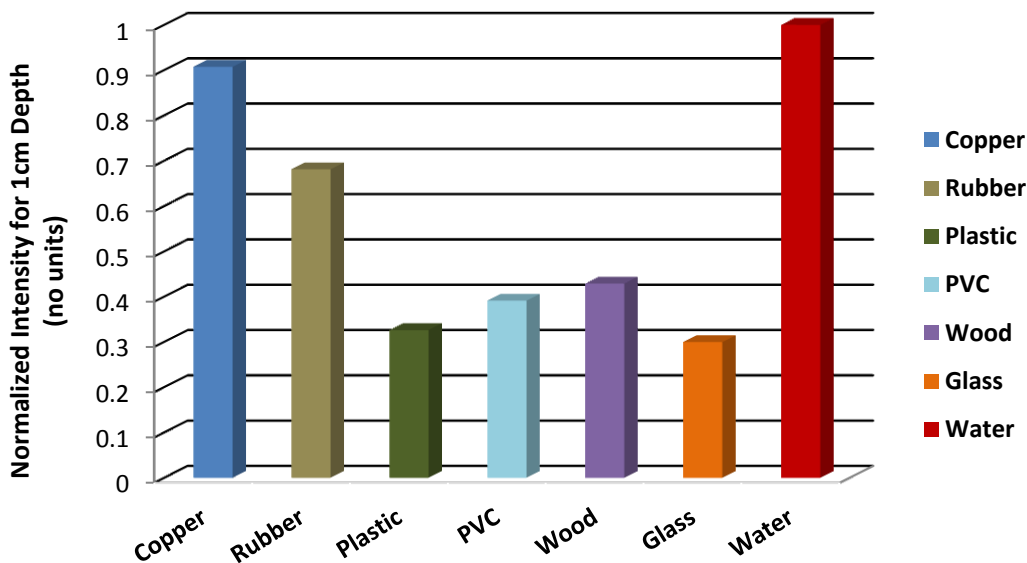


Figure 5-13: Intensity of different Materials for antenna at a distance of 1cm

Figure 5-13 shows the normalized Intensity for the different materials when the antenna is placed 1cm from the tumor. The bar graph in Figure 5-13 is made from the results for different materials (Copper, Rubber, Plastic PVC, Wood, Glass, Water) obtained in section 5.2 to compare the intensity level of materials with each other, in which Water has the highest intensity due to the high dielectric contrast between normal tissue (air) and tumor (Water) as compared to other materials.

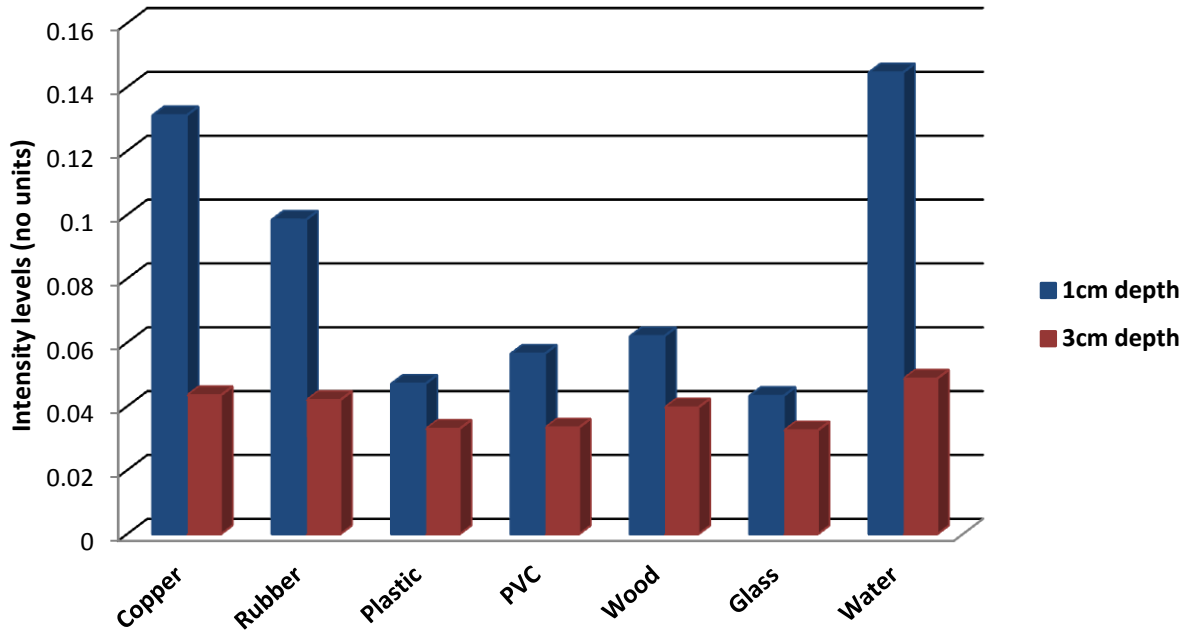


Figure 5-14: Comparison of Intensities of materials at 1cm & 3cm depth of tumor

Figure 5-14 compares the level of intensities for different distances of antenna i.e. 1 cm and 3 cm from tumor. It can be noted that as the distance is increased the level of intensity recorded at the antenna is reduced because when the antenna was placed 1 cm from the tumor, the signal strength is more as compared to when the antenna was placed 3cm from the tumor. The signal level got reduced due to the increase in the distance. Figure 5-15 represents the signal strength received at the antenna with respect to distance (1cm and 3cm) when antenna is exposed to water as tumor in environment.

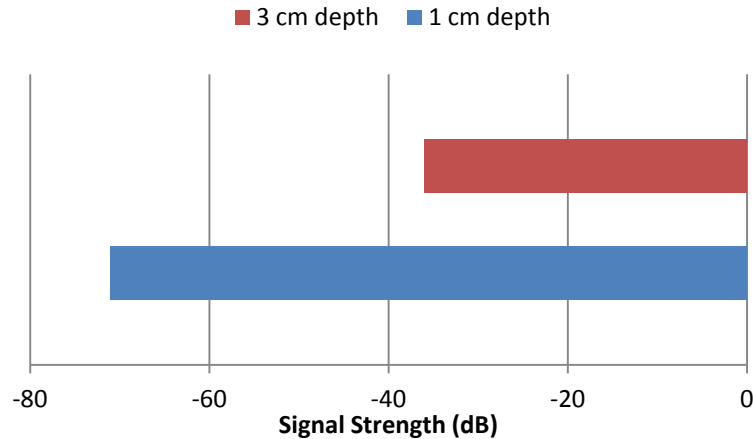


Figure 5-15: Signal strength received at the antenna for water as tumor at 1cm and 3cm depth

Apart from being computationally robust, Confocal Microwave Imaging algorithm led to certain underestimations in terms of the size of the tumor. This is due to the averaging method during the clutter removal process as discussed in chapter 4. Averaging as proposed by Hagness et al. is used to remove the antenna reflections from the backscattered signal [13]. In this method, the average of the backscattered responses from several antenna positions is subtracted from the response of each antenna position.

For the averaging method, it is assumed that the response of the environment at different antenna positions is similar since the environment is assumed to be symmetric, and that when the signals (response from the environment) are averaged, the similar signal levels will add up coherently. And the response received from the tumor differs in amplitude at different antenna positions, hence when the averaging is performed the tumor responses will add incoherently. Since the tumor response is at different time instants for different antenna positions due to the difference in the relative distance of the tumor to each antenna position, the tumor response adds incoherently in the averaging process and therefore it is suppressed in the average signal. All this is assumed that the environment signal is symmetric.

But this is not always the case, since the signals from the environment are not always symmetric which cause distortion to the possible tumor reflection (response). Hence when the averaging is performed the tumor and environment responses from all the antenna position are added and averaged incoherently. Consequently an unwanted averaged signal of the clutter (unwanted signal) and tumor response is added to each signal at the antenna position which weakens the tumor response and is undesirable.

Another problem of the averaging is that if the tumor is approximately equidistant to some of the antenna positions in the array, the processed signal (the signal that is received after averaging) will have high attenuation. This will make the tumor detection very difficult or even impossible.

We have calculated the time delays using the electrical permittivity of the air ϵ_r which is 1 for the case of our experiment. Since our model was a single layer model, it was easier to determine the value of ϵ_r to calculate the time delays. However, if we go to multilayer breast models the interaction of ϵ_r will subsequently change and it is hard to determine ϵ_r of the other layers besides that of the skin. The skin's dielectric permittivity can be determined by using the dielectric probe, but the permittivity of the fats in a women breast is undetermined, which may cause underestimations in location and size of tumor, which is reported by Salvador et al in [39].

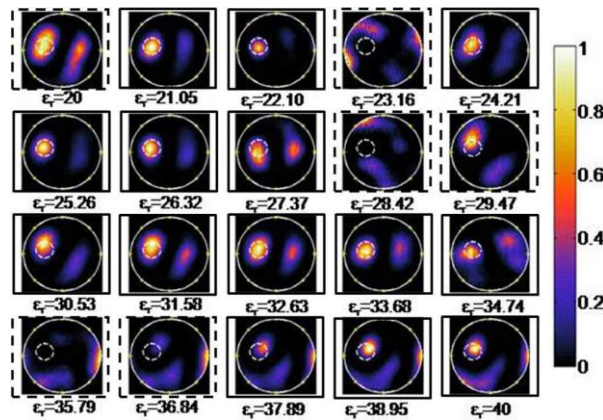


Figure 5-16: Effect of permittivity of medium in detection tumor using Confocal Algorithm [39]

The Figure 5-16 is taken from [39] which shows the results obtained from the experiment performed by Salvador et al. The Fig illustrates that as the dielectric permittivity is changed, the location and size of the tumor is changed, which is a limitation in confocal microwave imaging algorithm. The results obtained from our experiment shows that the Confocal Microwave Imaging algorithm can effectively detect tumor to a depth of 3cm, by taking certain assumptions, such as the considering the normal tissue to be homogenous. The effectiveness of confocal microwave imaging algorithm is shown through the results with the detection of tumor in Figure 5-6 to Figure 5-12, however due to the averaging method and assumptions for the permittivity of the dielectric medium may limit the analysis for multiple tumor detection which will be considered in future experimental analysis at Durham University.

6 CONCLUSION & FUTURE IMPROVEMENTS

6.1 CONCLUSION

Microwave imaging for the detection of breast cancer has become one of the most important research interests in recent times. The recent developments in breast cancer detection and the reported discomforts along with the involvement of health risks from the currently used screening methods as discussed in section 2.4 & 2.5 has led to a creation of a screening tool that has the minimum amount of health risk; which is able to detect tumor in breast at its early stage; cost effective; provides minimum discomfort to the patients etc. The strong prospect for this is therefore the Microwave Imaging techniques for early detection of tumor.

Researchers have presented different techniques for clinical implementation of microwave imaging with research at Dartmouth College, the University of Wisconsin and the University of Calgary. Microwave imaging using Radar based detection of breast tumor presents a comfortable and a safe method for patients under test. The contrast in the dielectric properties of breast tissues, normal and cancerous tissues, is key feature for the detection of tumor using microwave signal.

As highlighted the incident electromagnetic field would scatter from the interfaces of the breast tissues, due to their dielectric differences and the collected backscattered signal are processed by a post processing algorithm to create an image map representing the inner of the breast. The post processing algorithm used is the Confocal Microwave Imaging Algorithm, where we present the results which signify the effectiveness and the limitations of the algorithm towards breast cancer detection. Microwave imaging techniques offer the potential of low cost, non-invasive screening tool and within a non-harmful spectrum range.

In this report, experimental results of UWB microwave imaging system for Radar based breast cancer detection is presented, whereby we confirm the detection of tumor with 10 - 20 mm diameter and producing the viability of using the confocal algorithm for early breast cancer detection. We analyze the Confocal Microwave Imaging Algorithm for different permittivity of materials to investigate its effectiveness.

The results show that the materials i.e. water, silicon, PVC, copper, rubber, wood, glass and plastic used in the experiment tend to generate more scatter in the surrounding due to difference in electrical conductivity between each of them. The results also show that the level of intensity changes when the distance of the antenna is changed from 1cm to 3cm from the materials (tumor), because of the low power level recorded as the signal is received.

The results also signify the effect of the electrical permittivity in contrast between the normal and cancerous tissue. Due to the increase in the ratio of the dielectric contrast, different materials give more scatter, with water having a higher dielectric ratio with air giving a higher amount of scatter and PVC with a lower dielectric ratio with air recording a lower amount of scatter at the antenna. If the amount of additional scatter is more, then the size of the tumor located will be affected which will generate problems in identifying the actual size of tumor.

The results signify that the distance of the antenna from the tumor and the permittivity of the medium directly affects the location and the size of the tumor when Confocal Microwave Imaging algorithm is considered. Although the algorithm used for our experimental work is computationally simple but it has limitations, such as it provides limited performance in terms of image resolution and clutter rejection.

6.2 FUTURE IMPROVEMENTS

- A breast model to simulate a real breast tissue, using varying permittivity of tumor tissues to establish the base of Confocal Microwave Imaging Algorithm as the prime tumor detection technique for microwave imaging.

- Unlike mono-static antenna, a multi static antenna gives better approximations, since it is capable of gathering more data. Experimental setup using a set of antenna array for corrective readings and measurements for multiple positions to save time and to construct the basis for future research into breast cancer detection at Durham University as that of the Dartmouth College and University of Wisconsin.

- A tumor tissue has different permittivity levels to that of skin and air. In the experiment above, only the permittivity of the air is considered and the time delay is thus recorded. The exact time delay can be calculated by subtracting the total time delay with the backscatter that arrives at the antenna with air and skin as discussed in [41], resulting in the exact location of the tumor.

7 REFERENCES

- [1] Cancer Research UK [online] (2011) Available from: <http://info.cancerresearchuk.org> [accessed 15th June 2011].
- [2] Hu Y p, Wang Y d. Study on prevalence status qou and trend of women breast cancer in putuo district[J]. Shanghai Health Education And Health Promotion, 2007, 2(1):7-24,
- [3] Fear C, Hagness S C, Meaney P M, et al. “Enhancing breast Tumor detection with near field imaging” [J]. IEEE Microwave Magazine 2002,3(1): 48-56
- [4] OI H R, Diakidies N A. Thermal infrared imaging in early breast Cancer detecion- A survery of recent research [C]//25th Annual International Conference of IEEE on Engineering in Medicine and Biology Society, Piscataway: IEEE, 2003, 2 (17/21): 1109- 112.
- [5] Bindu G,lonappan A.thomas V, et al. Active microwave imaging For breast cancel detection[J]. Progress in Electromagnetics Research PIER, 2006, 58L:149-169.
- [6] Osen A. Stuchly M A,Vorst A V.Applications of RF/Microwaves in medicine (J). IEEE Trans. On Microwave . Theory tech, 2002,,50:963-974
- [7] E. J. Bond, X. Li, S. C. Hagness, B.D. Van Veen, “Microwave Imaging via Space-Time Beamforming for Early Detection of Breast Cancer”, IEEE Trans. Ant. Propag., vol. 51, no. 8, Aug. 2003.
- [8] X. Li and S.C. Hagness, “A confocal microwave imaging algorithm for breast cancer detection,” IEEE Microwave Wireless Components Lett., vol. 11, pp. 130-132, Mar. 2001.
- [9] Fear E C, Sill J M, Preliminary investigation of tissue sensing adaptive Radar for breast tumor detection{C}// Proceeding of the 25th Annual Meeting of the IEEE Engineering in Medicine and Biology Society, Piscatawau: IEEE, 2003:3787-33890
- [10] Maciej Klemm, Ian J. Craddock, Jack A. Leendertz, Alan Preece, and Ralph Benjamin” Radar-Based Breast Cancer Detection Using a Hemispherical Antenna Array—Experimental Results” IEEE transactions on antennas and propagation, vol. 57, NO. 6, JUNE 2009
- [11] A. J. Surowiec, et al., "dielectric-properties of breast-carcinoma and the surrounding tissues," Ieee Transactions on Biomedical Engineering, vol. 35, pp. 257-263, 1988
- [12] Committee on Technologies for the Early Detection of Breast Cancer, Mammography and Beyond: Developing Technologies for the Early Detection of Breast Cancer, S.J. Nass, I.C. Henderson, and J.C. Lashof, Eds. National Cancer Policy Board, Institute of Medicine, and Commission on Life Studies, National Research Council, 2001.

- [13] Elise C. Fear*, Member, IEEE, Xu Li, Student Member, IEEE, Susan C. Hagness, Member, IEEE, and Maria A. Stuchly, Fellow, IEEE “Confocal Microwave Imaging for Breast Cancer Detection: Localization of Tumors in Three Dimensions” IEEE Transactions on biomedical engineering, vol. 49, NO. 8, AUGUST 2002

- [14] S.C. Hagness, A. Taflove, and J.E. Bridges, “Two-dimensional FDTD analysis of a pulsed microwave confocal system for breast cancer detection: fixed-focus and antenna-array sensors”, IEEE Trans. Biomed. Eng., vol. 45, pp. 1470-1479, Dec. 1998.

- [15] Novant Medical Group [online] (2011) Available from: <http://www.novantmedicalgroup.org> [accessed 15th June 2011].

- [16] National Cancer Institute [online] (2011) Available from: <http://www.cancer.gov> [accessed 15th June 2011].

- [17] Caring for Cancer [online] (2011) Available from: www.caring4cancer.com [accessed 15th June 2011].

- [18] T. S. England and N. A. Sharples, "Dielectric properties of the human body in the microwave region of the spectrum," Nature, vol. 163, pp. 487-488, 1949.

- [19] T. S. England, "Dielectric properties of the human body for wavelength in the 1-10 cm range," Nature, vol. 1466, pp. 480-481, 1950.

- [20] D.J. Watmough and K.M. Quan, “X-ray mammography and breast compression”, *Lancet*, 340, p.122, 1992.

- [21] D. D. Stark and W. G. Bradley, Jr., Magnetic Resonance Imaging, 2nd ed., Mosby-Year Books, St. Louis, 1992.

- [22] M. A. Brown and R. C. Semelka, MRI: Basic Principles and Applications, 2nd ed., Wiley-Liss, New York, 1999.

- [23] S. C. Bushong, Diagnostic Ultrasound, McGraw-Hill, New York, 1999.

- [24] D. Paquette, J. Snider, F. Bouchard, I. Olivotto, H. Bryant, K. Decker, and G. Doyle, “Performance of screening mammography in organized programs in Canada in 1996,” Can. Med. Assoc. J., vol. 163, pp. 1133-1138, 2000.

- [25] M. L. Finkel, Understanding the Mammography Controversy: Science, Politics, and Breast Cancer Screening, 1st edition, Greenwood Publishing Group, Inc., 2005.

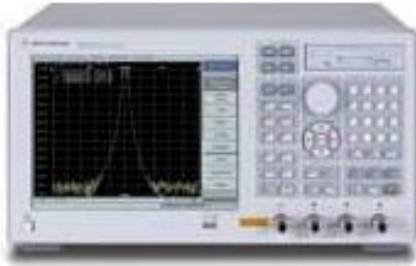
- [26] Breast Health Online [online] (2011) Available from: <http://www.imaginis.com/breasthealth> [accessed 20th June 2011].

- [27] Emorial Hospital of Texas County [online] (2011) Available from: <http://www.mhtcguymon.org/> [accessed 20th June 2011].
- [28] S.C. Hagness, A. Taflove, and J.E. Bridges, “Three-dimensional FDTD analysis of pulsed microwave confocal system for breast cancer detection: design of an antenna-array element”, IEEE Trans. Antennas Propagat., vol. 47, pp. 783-791, May 1999.
- [29] E.C. Fear and M.A. Stuchly “Microwave detection of breast cancer,” IEEE Trans Microwave Theory Tech., vol. 48, pp. 1854-1863, Nov. 2000.
- [30] E.C. Fear and M.A. Stuchly, “Microwave system for breast tumor detection,” IEEE Microwave Guided Wave Lett., vol. 9, pp. 470-472, Nov. 1999.
- [31] Xu Li, Student Member, IEEE, and Susan C. Hagness, Member, IEEE “A Confocal Microwave Imaging Algorithm for Breast Cancer Detection” IEEE microwave and wireless components letters, vol. 11, NO. 3, MARCH 2001
- [32] P. Meaney, S. Pendergrass, M. Fanning, D. Li, and K. Paulsen, “Importance of using a reduced contrast coupling medium in 2D microwave breast imaging,” Journal of Electromagnetic Waves and Applications, vol. 17, no. 2, pp. 333–355, 2003.
- [33] P. Meaney, M. Fanning, D. Li, S. Poplack, and K. Paulsen, “A clinical prototype for active microwave imaging of the breast,” IEEE Transactions on Microwave Theory and Techniques, vol. 48, no. 111, pp.1841–1853, 2000.
- [34] P. Meaney, K. Paulsen, J. Chang, and M. Fanning, “Initial microwave imaging experiments in ex-vivo breast tissue,” Proceedings of the First Joint BMES/EMBS Conference, 1999, vol. 2, p. 1130, 1999.
- [35] D. Li, P. Meaney, T. Raynolds, S. Pendergrass, M. Fanning, and K. Paulsen, “A broadband microwave breast imaging system,” Proceedings of the IEEE 29th Annual Bioengineering Conference, 2003, pp. 83–84, 2003.
- [36] S. K. Davis, X. Li, E. J. Bond, S. C. Hagness, B. D. Van Veen, “Frequency-Domain Penalized Least-Squares Beamformer Design for Early Detection of breast Cancer via Microwave Imaging”, Sensor Array and Multichannel Signal Processing Workshop Proceedings, pp. 120 – 124, Aug. 2002.
- [37] X. Li, S. K. Davis, S. C. Hagness, D. W. van der Weide, and B. D. Van Veen, “Microwave imaging via space-time beamforming: experimental investigation of tumor detection of multilayer breast phantoms,” IEEE Trans. Microwave Theory and Tech., vol. 52, pp 1856-1865, Aug. 2004.

- [38] X. Li, E. J. Bond, B. D. Van Veen, and S. C. Hagness, "An overview of ultrawideband microwave imaging via space-time beamforming for early-stage breastcancer detection," *IEEE Ant. Prop. Mag.*, Vol. 47, pp. 19-34, Feb. 2005.
- [39] Sara M. Salvador, Giuseppe Vecchi, "Experimental Tests of Microwave Breast Cancer Detection on Phantoms", *IEEE* 2009
- [40] S.M. Salvador, G. Vecchi, G.Pagana, C.Cacciatore, R.Maggiora, E.Attardo, "A comparison between two algorithms for microwave breast cancer detection" ,LACE/DELEN, Politecnico di Torino, C.so Duca degli Abruzzi 24, 10129 Torino, Italy.
- [41] A. Lazaro, D. Girbau, and R. Villarino" simulated and experimental investigation of microwave imaging using uwb" *Progress In Electromagnetics Research, PIER* 94, 263 {280, 2009
- [42] Dielectric of various materials [online Available from: <http://www.thelenchannel.com/1dielectric.php> [accessed 20th June 2011].
- [43] Z.A. Sattar and S. Salous , "Experimental analysis of Confocal Algorithm using different approximations for UWB radar based breast cancer detection", presented at the Festival of radio science,University of Liecester Jan 2011.
- [44] D. W. Winters, J. D. Shea, E. L. Madsen, G. R. Frank, B. D. Van Veen, S. C. Hagness, "Estimating the Breast Surface using UWB Microwave Monostatic Backscatter Measurements" *IEEE Trans. Biomed. Eng.*, vol. 55, no. 1, pp. 247 –256, Jan.
- [45] D. W. Winters, B. D. Van Veen, and S.C. Hagness, "UWB Microwave Imaging for Breast Cancer Detection: An Algorithm for Estimating the Breast Surface", *IEEE Ant. Prop. Symp.*, pp. 267 - 270, July 2006.
- [46] Vitaliy Zhurbenko, "Challenges in the Design of Microwave Imaging Systems for Breast Cancer Detection", *Advances in Electrical and Computer Engineering, Volume 11, Number 1*, 2011

APPENDIX A: EXPERIMENTAL SETUP COMPONENT PICTURES

Both VNA (E5071A) and Calibration Kit



VNA E5071

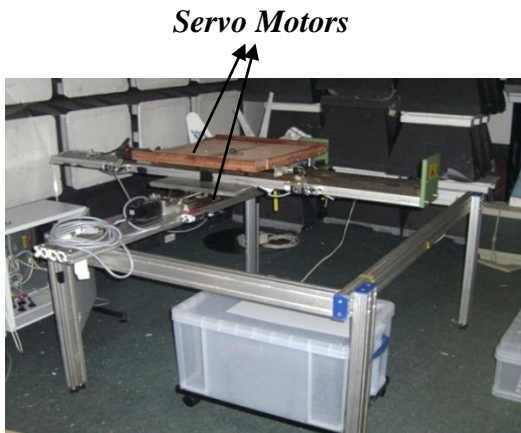


Calibration Kit

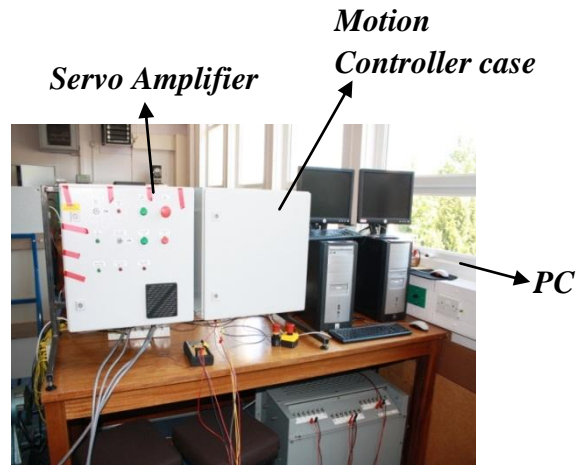


SMA Cable 50 Ω

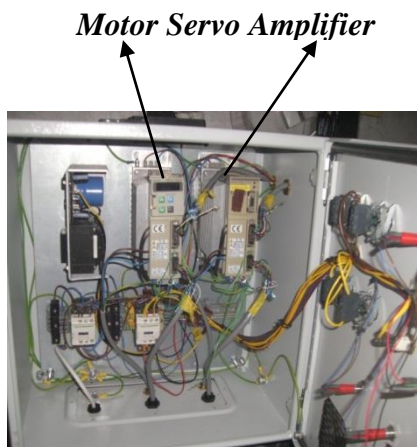
X – Y Probe and its Control Devices



X – Y Positioner

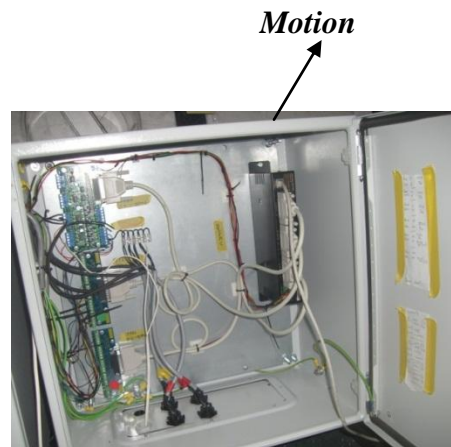


X-Y Probe Control Devices



Motor Servo Amplifier

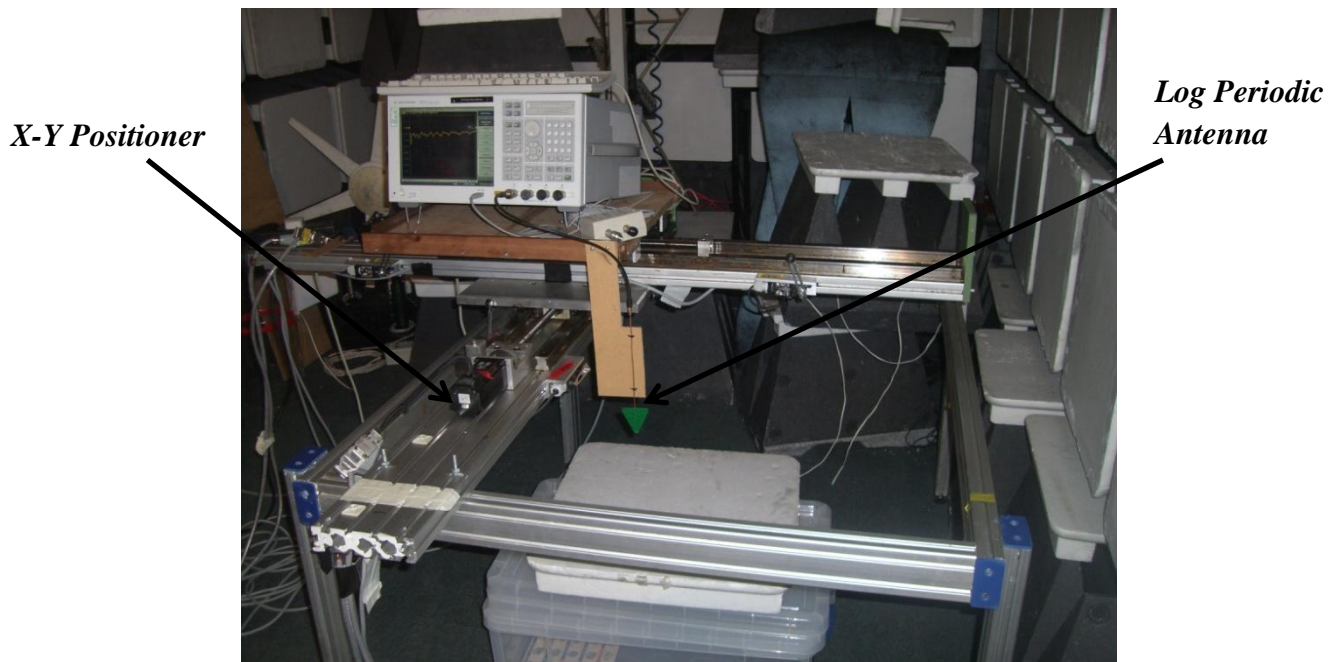
Servo Amplifier case



Motion

Motion controller case

Experimental Analysis on Effectiveness of Confocal Algorithm for Radar Based Breast Cancer Detection



Experimental Setup for Tumor Detection Using Confocal Microwave Imaging Algorithm



Materials Used as Tumor for Experimental Analysis

APPENDIX B: MATLAB CODES

`function ConfocalAlgorithm(With,Without,Frequency)`

```
%% WINDOWING
rows = 1601; cols = 36;
Window=hamming(1601);

Without_window = zeros(rows,cols);
With_window = zeros(rows,cols);

for k = 1:cols

    Without_window(:,k) = Without(:,k).*Window;
    With_window(:,k) = With(:,k).*Window;

end

TimeResolution = (rows-1)/(max(Frequency(:,1)) - min(Frequency(:,1)));

SampleSize = TimeResolution/(rows-1);

Time = linspace(-(rows-1)/2*SampleSize,(rows-1)/2*SampleSize,1601);
IFFT_Without= ifftshift (ifft(Without_window));
IFFT_With = ifftshift(ifft(With_window));
```

```
%% CALIBRATION
Calibrated_With = IFFT_With – IFFT_Without;

%% REMOVAL OF CLUTTER
Average = zeros(rows,6);

l = 1;

for k = 1:cols

    Average(:,l)= Average(:,l) + Calibrated_With(:,k);

    if (rem(k,6)==0)
        l = l+1;
    end

end
```

```
Average = Average./6;

New_With = zeros(rows,cols);
l = 1;
for k = 1:cols

    New_With(:,k) = Calibrated_With(:,k) - Average(:,l);

    if(rem(k,6)==0)
        l=l+1;
    end

end

RemovedSignal = abs(New_With);
```

```
%% DISTANCE OF ANTENNA LOCATION FROM EACH FOCAL POINT
[a,b] = meshgrid(linspace(0,10,6),linspace(0,10,6));

AntennaDistance = 1;

AntennaLocations_x = b(:)';
AntennaLocations_y = a(:)';

MAX = 256;

[X,Y]=meshgrid(linspace(-5,25,MAX),linspace(-10,20,MAX));%-10:0.1:20);
X=X(:);
Y=Y(:);
Distance = zeros(length(X),cols);

for k = 1:cols

    for m = 1:length(X)

        D1 = sqrt((AntennaLocations_x(k) - X(m) )^2 + (AntennaLocations_y(k) - Y(m) )^2);

        Distance(m,k) = sqrt(D1^2 + AntennaDistance^2);

    end

end
```

%% TIME VALUES FOR ANTENNA DISTANCE FROM EACH FOCAL POINT

```
Er = 1;  
vdelt = 3e10/sqrt(Er);  
  
TmR=zeros(length(X),cols);  
  
for k=1:cols  
    for l=1:length(X)  
        TmR(l,k)=2*Distance(l,k)/vdelt ;  
    end  
end
```

%% INTERPOLATION

```
InterpolatedData = zeros(length(TmR),cols);  
  
for k = 1:cols  
    InterpolatedData(:,k) = interp1(Time,RemovedSignal(:,k),TmR(:,k),'spline');  
end
```

%% INTENSITY VALUES

```
IntensityValues=zeros(length(InterpolatedData),1);  
  
for i=1:length(InterpolatedData)  
    IntensityValues(i)=sum(InterpolatedData(i,:));  
end  
  
IntensityValues=IntensityValues./max(IntensityValues);  
Intensity=IntensityValues.^4;
```

%% IMAGE

```
figure;  
  
scatter(X,Y,500,(Intensity),'!');  
axis([min(X) 22 min(Y) max(Y)]);
```

APPENDIX C: PRESENTED PAPER & CERTIFICATE IN URSI FESTIVAL 2011

Experimental analysis of Confocal Algorithm using different approximations for UWB radar based breast cancer detection

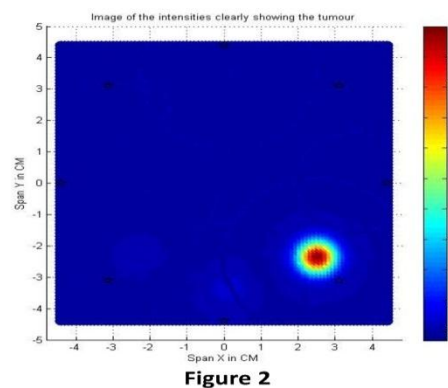
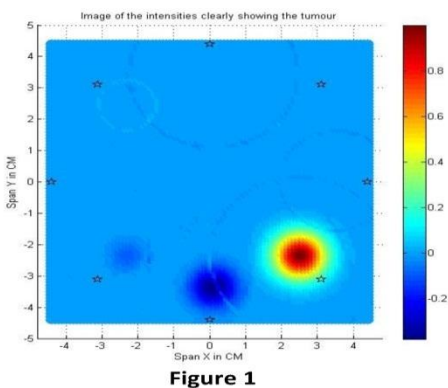
Z.A. Sattar and S. Salous
School of Engineering and Computing Sciences
Durham University

Abstract

The spreading of breast cancer worldwide and the need to develop new technologies to alleviate the tumour detection capability, present a challenge with the currently used imaging modalities. X-Ray, Ultrasound and MRI are the well-known imaging methods used for breast cancer detection. These have been reported to have adverse effects to the breast tissues, causing other diseases therein.

Presently, ultra wideband (UWB) radar based microwave imaging techniques are being used by most researchers due to its non-ionizing radiation, high accuracy, low cost and convenient for patients. In this technique, the breast is illuminated with an UWB pulse, and the backscattered signals are measured and then analysed using the Confocal Algorithm. A considerable challenge lies in reducing the amount of clutter.

In this presentation we present our experimental set up for breast cancer imaging studies which consists of a vector network analyser and a hand-made breast phantom. Using numerical data generated with the VNA, we apply the confocal algorithm to the data and analyse the results using different approximations to verify its ability to estimate a tumour response. Figure 1 and Figure 2 shows that the tumour of 1 cm diameter was correctly detected, while reviewing that the choice of using different approximations proved to suppress the clutter but affected the expected size of the tumour [1], [2].



-
- [1] Sara M. Salvador and Giuseppe Vecchi, " Experimental Tests of Microwave Breast Cancer Detection on Phantoms". IEEE Transactions on antennas and propagation, vol. 57, no. 6, june 2009.
 - [2] Elise C. Fear*, Xu Li, Susan C. Hagness, Maria A. Stuchly, Fellow, "Confocal Microwave Imaging for Breast Cancer Detection: Localization of Tumors in Three Dimensions". IEEE Transactions on biomedical engineering, vol. 49, no. 8, august 2002.



FESTIVAL OF RADIO SCIENCE

University of Leicester

12th January 2011

Miss Zubaida Abdul Sattar

presented her paper

Experimental analysis of Confocal Algorithm using different approximations
for UWB radar based breast cancer detection

Professor Andy Marvin FIET IEEE Fellow

Technical Director, York EMC Services Ltd.

York **EMC** Services Ltd